

UNIVERSIDAD DE BARCELONA
Facultad de Farmacia
Departamento de Bioquímica y Biología Molecular

**REDESIGN OF CARNITINE ACETYLTRANSFERASE
SPECIFICITY BY PROTEIN ENGINEERING**

ANTONIO FELIPE GARCIA CORDENTE

2006

RESULTS

1. ISOLATION AND CLONING OF RAT CARNITINE ACETYLTRANSFERASE

1.1. ISOLATION OF RAT CARNITINE ACETYLTRANSFERASE

cDNA was prepared from rat testis mRNA and rat CrAT was amplified by PCR using *Pfu* Turbo DNA polymerase with the following primers: CrAT-ATG.for and CrAT-2100.rev (see appendix for primer sequences). The sequence for CrAT-ATG.for was taken from a rat CrAT DNA sequence (GenBank XM_242301) and contains the ATG start codon and CrAT-2100.rev was designed from a rat cDNA clone that corresponds to the 3'-untranslated region of rat CrAT (GenBank AA925306). A fragment of 2070 nucleotides was obtained by PCR, purified and subcloned into the pGEM[®]-T vector, yielding the pGEM-T-CrAT^{wt} construct. The rat CrAT cDNA fragment was then sequenced and the nucleotide sequence was deposited in GenBank (Accession number AJ620886) (Fig. 1).

Rat CrAT mRNA encodes a predicted mitochondrial precursor protein (CrAT mit.) of 626 amino acids with a molecular mass of 71 kDa. The protein shows 96 and 90% identity with CrAT from mouse and human, respectively. The N-terminal end of the primary translation product has a 21 amino-acid sequence before the second methionine, which is the putative first amino acid in peroxisomal CrAT (CrAT per.). Thus, the peroxisomal isoform would consist of 605 amino acids. By comparison with other CrATs we postulated a 29-amino acid sequence that would act as a mitochondrial targeting signal (MTS) (Corti, 1994b). Its amino acid composition is consistent with the general composition given for leader peptides that translocate cytosolic synthesized protein into mitochondria (Von Heijne, 1986). Rat CrAT also contains the C-terminal "AKL" peroxisomal targeting sequence (PTS).

Results

```
GGCATGGATGACCCCAAAGTGCCGGAGCAGCAGAGGGTGGAGCTGCTTCGAAAGGCTGTG      1500
G M D D P K V P E Q Q R V E L L R K A V

CAGGCCACCCGAGCCTACACCGACCGGCCATCCGAGGGGAGGCCTTTGACCGGCACTTG      1560
Q A H R A Y T D R A I R G E A F D R H L

CTGGGTCTGAAGCTACAGGCCATCGAGGACCTGGTGAGCATGCCTGACATCTTCATGGAT      1620
L G L K L Q A I E D L V S M P D I F M D

ACCTCCTACGCCATTGCCATGCACTTCAACCTTTCTACCAGCCAGGTCCCTGCCAAGACA      1680
T S Y A I A M H F N L S T S Q V P A K T

GACTGTGTCATGTCTCTCGGACCTGTGGTCCCAGACGGTTACGGCATCTGCTACAATCCC      1740
D C V M S F G P V V P D G Y G I C Y N P

ATGGAGGCCCATATCAACTTTTCCGTGTGAGCCTACAACAGCTGTGCTGAGACCAACGCT      1800
M E A H I N F S V S A Y N S C A E T N A

GCCCGCATGGCTCACTACTTGGAGAAAGCTCTGCTGGACATGCGCACCTTACTCCAGAAC      1860
A R M A H Y L E K A L L D M R T L L Q N

CACCCAGGGCCAAGCTCTGAAACCCAGGCCAGGCCTGCCCGTCCACAGCCAAGCCAC      1920
H P R A K L *
```

Fig. 1. **cDNA and amino acid sequence of rat carnitine acetyltransferase.** Boxed nucleotides correspond to the first start codon and the TGA stop codon. The second start codon is underlined. In the amino acid sequence, the peroxisomal targeting signal, AKL, is underlined and the putative cleavage site of the mitochondrial targeting signal is indicated by an arrow. The coding sequence comprises nt 1-1881. The deposited sequence (GenBank AJ620886) also contains nt 1921-2070 (not shown). CrAT mit. indicates mitochondrial CrAT; CrAT per., peroxisomal CrAT.

1.2. GENERATION OF EXPRESSION CONSTRUCTS

Rat CrAT cDNA was cloned into two expression plasmids: pYES and pGEX-6P-1. The pYES plasmid is used for high-level expression of recombinant proteins in *S. cerevisiae* under the control of the promoter *GALI*, which is induced by growth of yeast cells in medium containing galactose. The pGEX-6P-1 vector is used for inducible, high-level intracellular expression of genes in *E. coli* as fusions with GST.

1.2.1. Construction of plasmids for expression in yeast

In order to study the kinetic properties of rat CrAT, the 1925 nt fragment containing the rat CrAT coding region was subcloned into the yeast expression plasmid pYES. To enable cloning into the only *HindIII* site of the plasmid, a *HindIII* site (underlined in the forward primer) was introduced immediately 5' of the first start codon by PCR, using pGEM-T-CrAT^{wt} as template. A consensus sequence (in boldface type) optimized for efficient translation into yeast was also introduced in the same PCR using

the forward primer *HindIII*-CrAT.for (5'-TCGATAAAGCTTTATAAAATGTTAGCCTTTGCTGCCAGAAC-3') and the reverse primer *EcoRI*-CrAT.rev (5'-CGGAATTCCGCCAAAGTGGGCTTGGCTGTG-3'), which introduces an *EcoRI* site (underlined). PCR products were digested with *HindIII* and *EcoRI* and ligated to the pYES plasmid, producing pYESCrAT^{wt}. This construct encodes the 626 amino-acid mitochondrial precursor CrAT protein. The rat CrAT cDNA insert was sequenced to rule out any PCR-introduced errors, as described in Materials and Methods (Section 2.12.)

1.2.2. Construction of plasmids for expression in *E. coli*

To express the full-length rat CrAT protein in *E. coli*, a cDNA fragment containing CrAT was obtained from plasmid pYESCrAT^{wt}, digested with *HindIII*, blunt-ended, and again digested with *EcoRI*. This fragment was then purified and subcloned into the expression vector pGEX-6P-1 previously digested with *BamHI*, blunt-ended and again digested with *EcoRI*. The plasmid obtained was pGEX-CrAT^{wt}. Rat CrAT protein was expressed in *E. coli* in order to purify the enzyme for the generation of anti-rat CrAT antibodies.

2. GENERATION OF ANTI-RAT CARNITINE ACETYL TRANSFERASE ANTIBODIES

2.1. EXPRESSION AND PURIFICATION OF RAT CrAT IN *E. COLI*

For expression and purification of rat CrAT protein the Glutathione S-Transferase (GST) Gene Fusion System was used. The pGEX-CrAT^{wt} construct was transformed into *E. coli* BL21 cells and the GST-CrAT fusion protein was overexpressed o/n after the addition of 0.1 mM IPTG at 18 °C. The soluble fusion protein was purified from bacterial lysates using Glutathione Sepharose 4B with a batch method. Finally, CrAT was eluted by cleavage of the fusion protein with *PreScission* protease. The yield of purified rat CrAT was typically 0.8 mg/L of culture. Purity of the enzyme was greater than 95% according to SDS-PAGE (Fig. 2). The molecular mass of purified CrAT estimated by SDS-PAGE was approximately 71 kDa, which corresponds to the mass of the full-length CrAT protein calculated from its amino acid sequence.

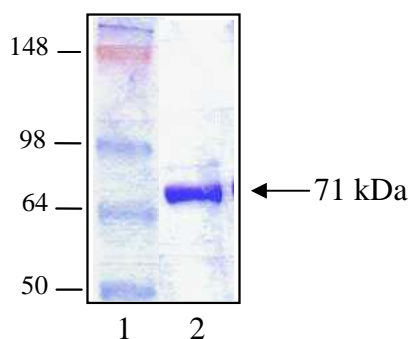


Fig 2. **SDS-PAGE of purified recombinant wild-type CrAT enzyme.** Protein samples were subjected to 8% SDS-PAGE and stained with Coomassie blue. *Lane 1* contains molecular mass marker. *Lane 2* contains 3 µg of purified wild-type CrAT. The arrow indicates the migration position and the molecular mass of rat CrAT.

2.2. GENERATION OF ANTIBODIES

To generate anti-rat CrAT antibodies, two female New Zealand White (NZW) rabbits were each injected subcutaneously on days 0, 21, 42, and 63 with 150 µg of the purified CrAT protein. The protein was emulsified 1:1 with Freund's complete adjuvant (day 0) or incomplete adjuvant (days 21, 42 and 63) in a total volume of 1 ml. Rabbits

were bled completely 10 days after the third booster (day 73) and then the serum with the anti-rat CrAT antibodies was isolated. All procedures were performed in accordance with the recommendations of the ethics committee for animal experimentation of the University of Barcelona.

To determine the optimal working dilution of the rabbit anti-rat CrAT primary antibody, mitochondrial protein from yeast expressing wild-type rat CrAT (Section 3.1.) was separated by SDS-PAGE and subjected to immunoblotting using different dilutions of the anti-rat CrAT antibody, ranging from 1:3,000 to 1:10,000. Goat anti-rabbit secondary antibody was applied at a 1:6,000 dilution. The optimal dilution of the primary antibody was found to be 1:10,000 (Fig. 3, lane 1). At this dilution, a strong, defined, and specific band of 71 kDa (determined by comparison with comigrating size markers) was observed. Lower dilutions of the primary antibody (1:3,000 and 1:6,000) resulted in a stronger signal, but at the same time produced a higher background signal and non-specific bands (data not shown). Anti-rat CrAT antibodies are specific to rat CrAT and they do not recognise yeast-expressed rat COT (Fig. 3, lane 2), even though both enzymes share 36% amino acid sequence identity. The absence of bands in lane 2 also indicates that the primary antibody does not recognise any endogenous yeast enzyme.

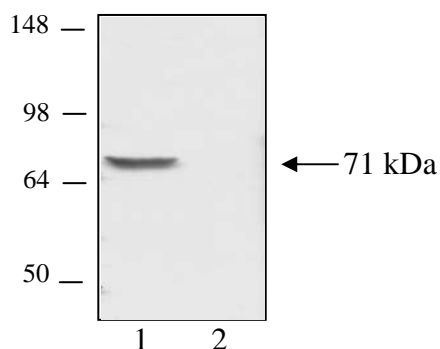


Fig. 3. Western-blot analysis of anti-rat CrAT antibody response to yeast-expressed rat carnitine acyltransferase proteins. Mitochondrial protein (8 μ g) from yeast expressing wild-type CrAT (lane 1) and COT (lane 2) were separated by 8% SDS-PAGE and subjected to immunoblotting using anti-rat CrAT antibodies. The arrow indicates the migration position and the molecular mass of the band recognised by the anti-rat CrAT antibodies.

3. EXPRESSION OF RAT CARNITINE ACETYLTRANSFERASE IN *SACCHAROMYCES CEREVISIAE*

3.1. USE OF *SACCHAROMYCES CEREVISIAE* AS AN EXPRESSION SYSTEM

S. cerevisiae was used as a heterologous expression system for carnitine acyltransferases. Yeast cells are devoid of endogenous COT and CPT activities but they do contain CrAT activity, so an *S. cerevisiae* strain lacking the endogenous *CAT2* gene (FY23 Δ *cat2* (MATa *trp1 ura3* Δ *cat2::LEU2*)) was used. Although this strain contains two additional CrAT genes, *YAT1* and *YAT2*, carnitine acetyltransferase activity was not detected under the conditions in which it was expressed in this study. The absence of carnitine acyltransferase activity in the FY23 Δ *cat2* strain facilitates the interpretation of the kinetic studies of the overexpressed proteins, whereas overexpression of carnitine acyltransferases in mammalian cells is not suitable for functional studies, as these cells have endogenous CrAT, COT and CPT activities. Previously, it has been demonstrated that the expression of murine L-CPT I (Prip-Buus, 1998) and COT (Morillas, 2000) in *S. cerevisiae* is a valid model to study the structure-function relationships of these proteins. Yeast-expressed rat L-CPT I and COT showed the same topological and biochemical properties as the native enzyme.

3.2. EXPRESSION OF RAT CARNITINE ACETYLTRANSFERASE IN YEAST

Plasmids pYES and pYESCrAT^{wt} were transformed in the *S. cerevisiae* strain FY23 Δ *cat2*. Uracil-positive (Ura⁺) transformants were selected and overexpression of rat CrAT was induced by growth of the cells on a galactose-containing medium, as described in Materials and Methods (Section 4.3.). The pYES vector alone was used as a negative control.

Yeast-expressed rat CrAT protein is expected to be targeted to the yeast mitochondrial matrix. The expressed protein contains both the MTS and PTS. It has been demonstrated in yeast (Elgersma, 1995) and mammals (Corti, 1994b) that in the presence of both signals, the MTS overrules the PTS, and the protein is targeted exclusively to

the mitochondria. To study whether rat CrAT is targeted to the mitochondria of transformed yeast, a cell homogenate was subjected to differential centrifugation to obtain a pellet enriched in mitochondria. CrAT activity was checked using a fluorometric method with acetyl-CoA as substrate, as described in Materials and Methods (Section 7.1). Approximately, 65% of total CrAT activity was found in the mitochondrial pellet fraction ($392 \text{ nmol}\cdot\text{min}^{-1}\cdot\text{mg protein}^{-1}$), whereas the remaining activity was present in the supernatant fraction ($250 \text{ nmol}\cdot\text{min}^{-1}\cdot\text{mg protein}^{-1}$). The relatively high activity observed in the supernatant was probably due to leakage of mitochondrial CrAT during the mitochondrial isolation process. Therefore, we used the mitochondrial fraction for further studies. No carnitine acetyltransferase activity was detected in control yeast transformed with the empty plasmid.

3.3. ACYL-GROUP SELECTIVITY OF RAT CARNITINE ACETYLTRANSFERASE EXPRESSED IN YEAST

Enzyme activity of yeast-expressed wt CrAT was tested for acyl-CoA substrates of various lengths ranging from acetyl- to palmitoyl-CoA (Fig. 4A). Wild-type CrAT was highly active toward acetyl-, propionyl- and butyryl-CoA, the latter being the optimal substrate. Activities toward longer acyl-CoAs decreased dramatically; for example, activity toward hexanoyl-CoA was only 22% of that with butyryl-CoA. CrAT activity was practically zero with lauroyl-CoA (C_{12} -CoA) and longer acyl-CoAs. CrAT showed a strong preference for short-chain acyl-CoAs as substrates.

Expression of rat CrAT in *S. cerevisiae* was confirmed by Western-blot analysis using rat CrAT-specific antibodies, as described in Section 2.2. Mitochondrial extracts from yeast cells transformed with pYESCrAT^{wt} showed a single band of about 71 kDa, which corresponds to rat CrAT (Fig 4B, lane 2), whereas no band was observed in cells transformed with the empty plasmid (Fig 4B, lane 1).

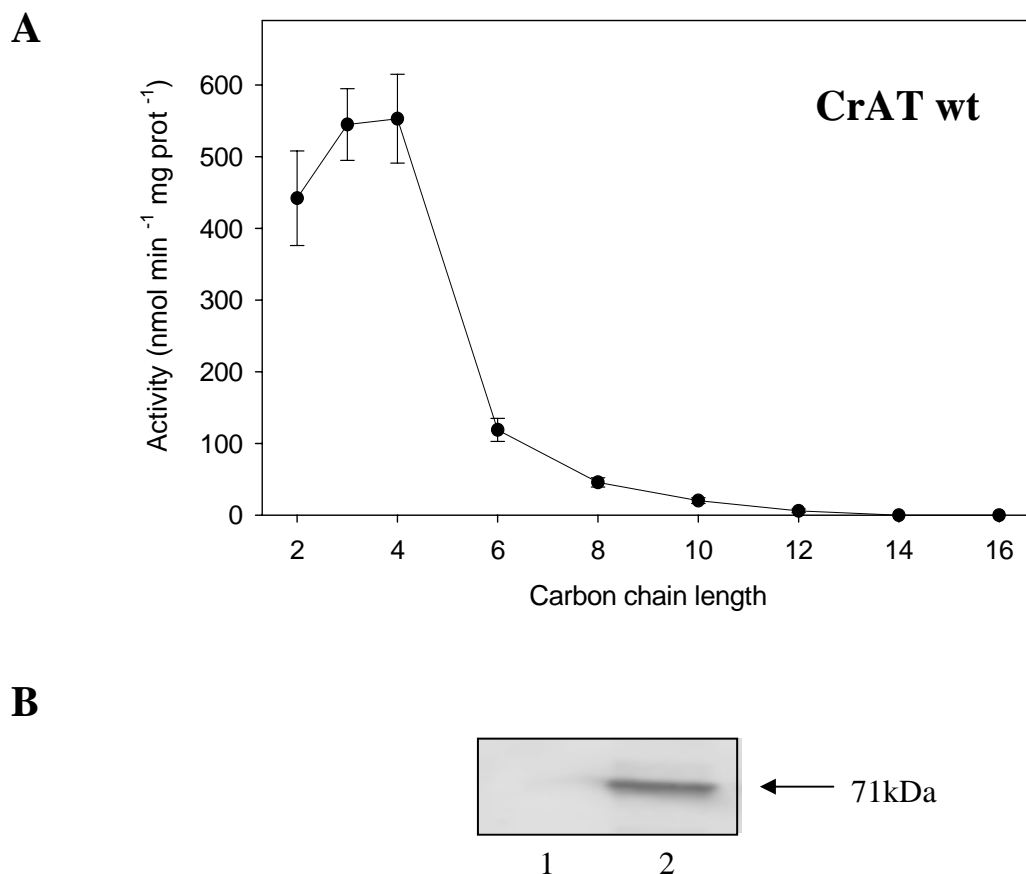


Fig. 4. **Carnitine acyltransferase activity in yeast cells expressing wt rat CrAT.** A) Mitochondrial extracts from yeast expressing wt CrAT were assayed for activity with acyl-CoAs of different carbon-chain lengths, ranging from C₂- to C₁₆-CoA. Results are shown as the mean \pm S.D. of at least three independent experiments. B) Immunoblot analysis of wt CrAT in *S. cerevisiae*. Yeast samples (8 μ g) were separated by 8% SDS-PAGE and subjected to immunoblotting using specific antibodies for CrAT. Lane 1, extracts from yeast transformed with the empty pYES plasmid; lane 2, wild-type CrAT. The arrow indicates the migration position and the molecular mass of rat CrAT.

3.4. KINETIC PROPERTIES OF RAT CARNITINE ACETYLTRANSFERASE EXPRESSED IN YEAST

A series of kinetic experiments was performed with wild-type CrAT by varying the length of the acyl-CoA substrate from acetyl- to octanoyl-CoA. It was not possible to determine kinetic parameters for acyl-CoAs longer than 8 carbons due to their low activity levels. Yeast-expressed rat CrAT showed standard saturation kinetics for both L-carnitine and acyl-CoA substrates (Fig. 5). This property was general for all acyl-CoAs, irrespective of their length (data not shown).

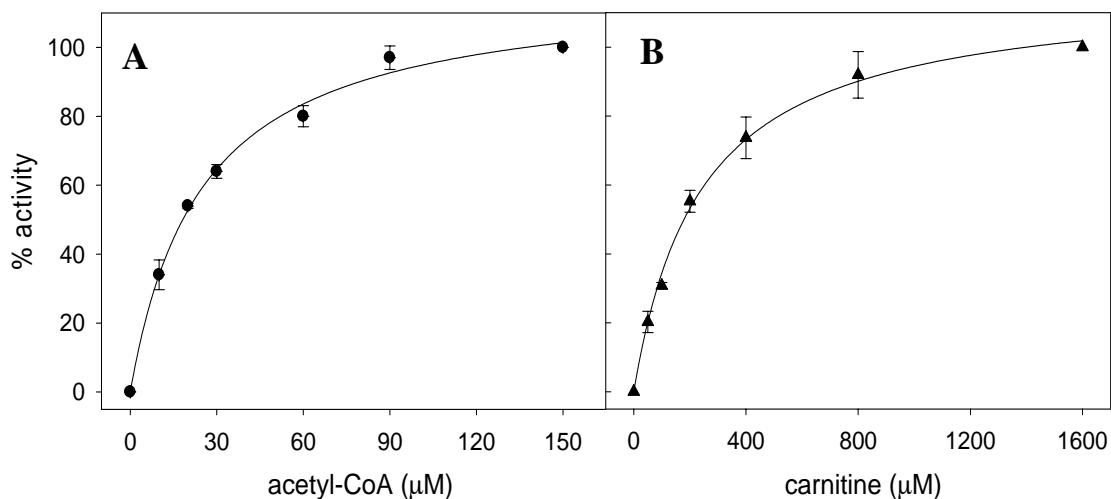


Fig. 5. **Carnitine and acetyl-CoA saturation curves for yeast-expressed CrAT.** Mitochondrial protein (5 μg) from yeast expressing CrAT was assayed for carnitine acyltransferase activity either at 1500 μM carnitine with increasing concentrations of acetyl-CoA (A) or at 100 μM acetyl-CoA with increasing concentrations of carnitine (B). The results are the mean \pm S.D. of at least three independent experiments.

K_m values for CrAT varied slightly (between 23 and 33 μM) with the chain length of the acyl-CoA substrate (Table 1). V_{max} was maximal for C₃-CoA (780 $\text{nmol}\cdot\text{min}^{-1}\cdot\text{mg protein}^{-1}$) and this parameter was also very high for C₂- and C₄-CoA (550 and 685 $\text{nmol}\cdot\text{min}^{-1}\cdot\text{mg protein}^{-1}$, respectively). V_{max} for acyl-CoAs longer than C₄-CoA decreased rapidly and for C₈-CoA was only 6% of that for C₃-CoA. Catalytic efficiency (defined as V_{max} / K_m) followed the same pattern as V_{max} , and maximum catalytic efficiency was observed for C₃-CoA.

Kinetic parameters using L-carnitine as substrate were also measured by varying the length of acyl-CoA (Table 1). The K_m increased with the length of the acyl-CoA substrate. For example, the K_m for carnitine with octanoyl-CoA was 5 times higher than that for acetyl-CoA (964 and 203 μM , respectively). Again, V_{max} and catalytic efficiency was maximal with C₃-CoA. When octanoyl was the substrate, V_{max} decreased to 6% compared with C₃-CoA. Catalytic efficiency for carnitine also decreased with the length of the acyl-CoA; for example, catalytic efficiency for octanoyl-CoA was only 2% compared with any of the short-chain substrates (from C₂- to C₄-CoA). This implies that short-chain acyl-CoAs are preferential substrates when the concentration of carnitine is low and that the binding of medium- and long-chain acyl-CoAs lowers the affinity for carnitine.

Results

Acyl-CoA	K_m		V_{max}		Catalytic efficiency	
	L-carnitine	acyl-CoA	L-carnitine	acyl-CoA	L-carnitine	acyl-CoA
	μM		$\text{nmol}\cdot\text{min}^{-1}\cdot\text{mg protein}^{-1}$		V_{max} / K_m	
C ₂ -CoA	203 ± 21	22.8 ± 1.0	515 ± 56	550 ± 99	2.53	24.1
C ₃ -CoA	281 ± 19	22.8 ± 1.6	880 ± 99	780 ± 16	3.14	34.2
C ₄ -CoA	220 ± 54	30.7 ± 2.8	567 ± 97	685 ± 85	2.58	22.3
C ₆ -CoA	567 ± 80	33.2 ± 4.6	176 ± 22	148 ± 5.1	0.31	4.46
C ₈ -CoA	964 ± 120	24.7 ± 6.5	53 ± 8.0	45.0 ± 7.1	0.05	1.82

Table 1. **Kinetic parameters of rat CrAT expressed in *S. cerevisiae*.** Mitochondrial protein (5 μg) from yeast-expressing wild-type CrAT was assayed with acyl-CoAs of different carbon-chain lengths ranging from acetyl- to octanoyl-CoA. Results are shown as the mean \pm S.D. of three experiments.

4. EXPRESSION OF RAT CARNITINE OCTANOYL TRANSFERASE IN YEAST

Rat liver COT cDNA had previously been isolated and cloned into the yeast expression plasmid pYES in our group (Morillas, 2000). The resulting pYESCOT^{wt} construct contains the coding region of rat COT and includes nt 52-2009 of the previously reported COT sequence U26033 (Choi, 1995).

The plasmid containing wild-type COT was transformed in the *S. cerevisiae* strain FY23 Δ cat2 and protein expression was induced by growth of positive transformants (Ura⁺) on a galactose-containing medium. Yeast extracts were obtained and assayed for COT activity using decanoyl-CoA and L-carnitine as substrates, as described in Materials and Methods (Section 7.1). Since it had been shown previously that COT activity was enriched in the pellet of the crude extracts (Morillas, 2000), we used this pellet fraction for further studies. COT activity with decanoyl-CoA as substrate was 556 $\text{nmol}\cdot\text{min}^{-1}\cdot\text{mg protein}^{-1}$, whereas in cells transformed with the empty plasmid, COT activity was not detected. Western-blot analysis of yeast-expressed COT was performed using specific antibodies for rat COT. These antibodies had previously been obtained in our group against a peptide (residues 344-360) of rat COT (Caudevilla, 1998). Crude extracts from

yeast cells transformed with the pYESCOT^{wt} plasmid showed a single band of 69 kDa that corresponded to the full-length rat COT protein (Fig 6B, lane 2). No band was observed in cells transformed with the empty plasmid (Fig 6B, lane 1).

4.1. ACYL-GROUP SELECTIVITY OF RAT CARNITINE OCTANOYLTRANSFERASE EXPRESSED IN YEAST

Enzyme activity of yeast-expressed wild-type COT was tested for acyl-CoA substrates of various lengths ranging from acetyl- to arachidoyl-CoA (C₂₀-CoA) (Fig. 6A). Wild-type COT exhibited a relatively broad substrate specificity, ranging from butyryl- to palmitoyl-CoA. COT was highly active toward medium-chain acyl-CoAs (hexanoyl-, octanoyl-, and decanoyl-CoA) but not toward other acyl-CoAs with either a shorter or a longer hydrocarbon chain.

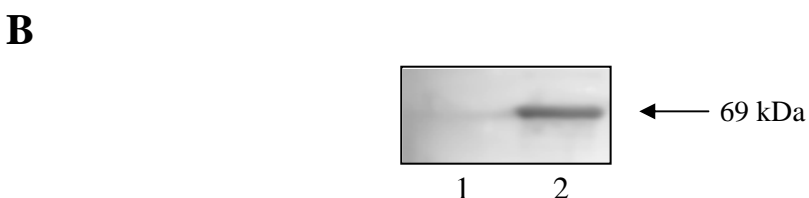
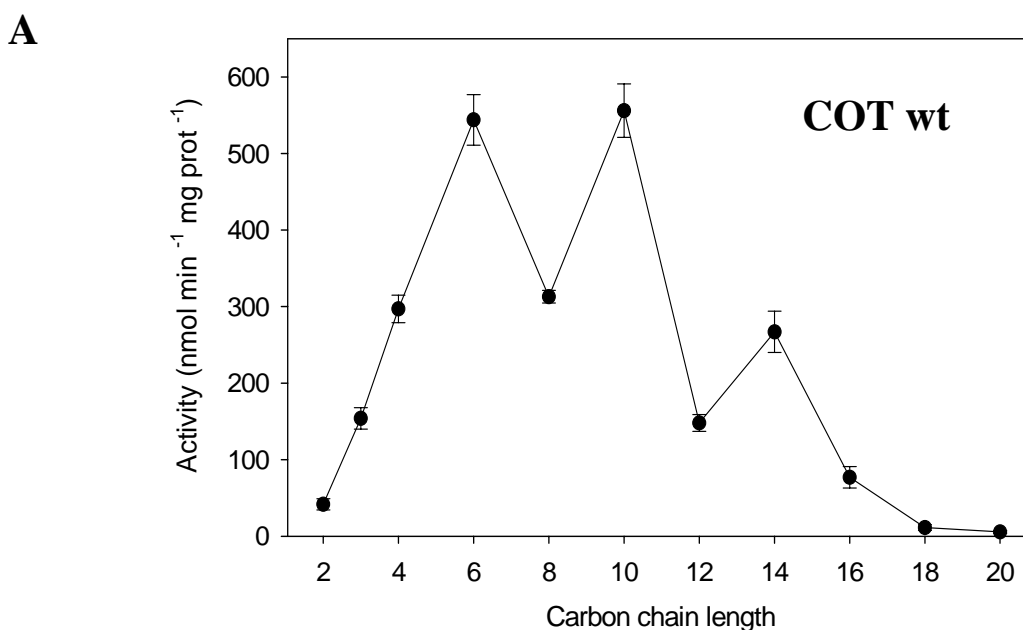


Fig. 6. Carnitine acyltransferase activity of yeast cells expressing wt rat COT. A) Crude extracts from yeast expressing wt COT were assayed for activity with acyl-CoAs of different chain length ranging from C₂- to C₂₀-CoA. Results are shown as the mean \pm S.D. of three experiments. B) Immunoblot analysis of recombinant wt COT in *S. cerevisiae*. Samples (10 μ g) were separated by 8% SDS-PAGE and subjected to immunoblotting using specific antibodies. Lane 1, extract from yeast transformed with the empty plasmid; lane 2, COT wild-type. The arrow indicates the migration position and molecular mass of rat COT.

4.2. KINETIC PROPERTIES OF RAT CARNITINE OCTANOYLTRANSFERASE EXPRESSED IN YEAST

A series of kinetic experiments were performed by varying the length of the acyl-CoA substrate from acetyl- to decanoyl-CoA (Table 2). Yeast-expressed rat COT showed standard saturation kinetics for both L-carnitine and acyl-CoA substrates (Fig. 7). This property was general for all acyl-CoAs, irrespective of their length (data not shown).

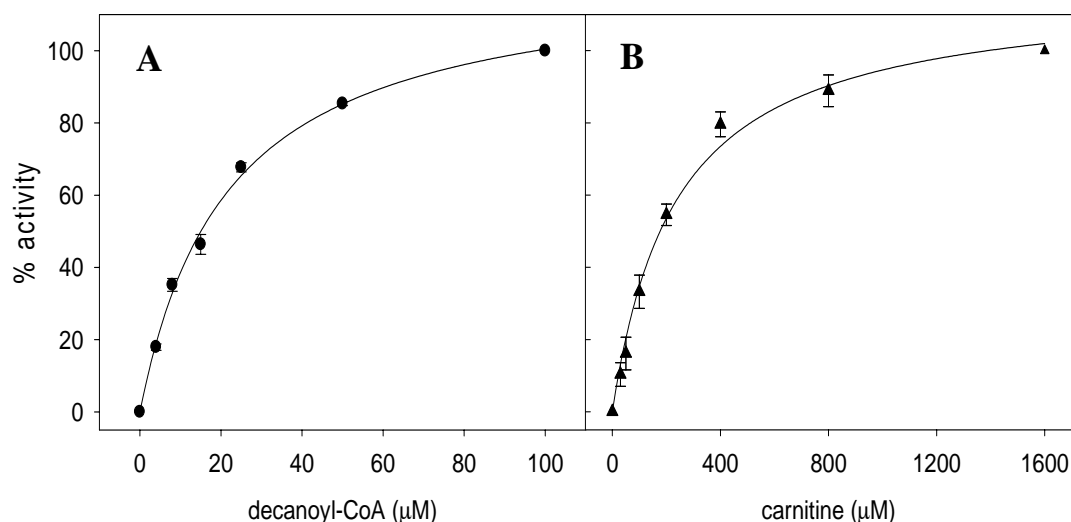


Fig. 7. **Carnitine and decanoyl-CoA saturation curves for expressed COT in *S. cerevisiae*.** Crude extracts (5 μg) isolated from yeast expressing COT were assayed for activity either at 1500 μM carnitine with increasing concentrations of decanoyl-CoA (A) or at 100 μM decanoyl-CoA with increasing concentrations of carnitine (B). Results are shown as the mean ± S.D. of at least three independent experiments

K_m values of yeast-expressed COT for acyl-CoA (Table 2) varied only slightly with the chain length of the substrate over the range C₂ to C₁₀ (12.7 ± 2.3 μM), as observed for yeast-expressed rat CrAT (see section 3.4). V_{max} was maximal for hexanoyl-CoA ($626 \text{ nmol}\cdot\text{min}^{-1}\cdot\text{mg protein}^{-1}$) and this value was also very high for decanoyl-CoA ($500 \text{ nmol}\cdot\text{min}^{-1}\cdot\text{mg protein}^{-1}$). Catalytic efficiency followed the same pattern as V_{max} , and maximum catalytic efficiency was observed for hexanoyl-CoA.

Kinetic parameters for L-carnitine were also measured but only with decanoyl-CoA as substrate. Under these conditions, the K_m for carnitine was 147 μM.

Results

Acyl-CoA	K_m		V_{max}		Catalytic efficiency	
	L-carnitine	acyl-CoA	L-carnitine	acyl-CoA	L-carnitine	acyl-CoA
	μM		$\text{nmol}\cdot\text{min}^{-1}\cdot\text{mg protein}^{-1}$		V_{max} / K_m	
C ₂ -CoA	-	13.0 ± 1.9	-	64 ± 4.0	-	4.91
C ₄ -CoA	-	8.9 ± 1.6	-	218 ± 18	-	24.6
C ₆ -CoA	-	15.0 ± 1.7	-	626 ± 26	-	42.0
C ₈ -CoA	-	13.0 ± 2.6	-	320 ± 38	-	24.6
C ₁₀ -CoA	147 ± 26	13.8 ± 2.9	430 ± 26	500 ± 88	2.92	36.2

Table 2. **Kinetic parameters of COT expressed in *S. cerevisiae*.** Crude protein extract (5 μg) from yeast expressing wt COT was assayed with acyl-CoAs of different carbon-chain lengths ranging from acetyl- to decanoyl-CoA. Results are shown as the mean \pm S.D. of three experiments.

5. FUNCTIONAL ANALYSIS OF CARNITINE ACETYL TRANSFERASE USING BIOINFORMATIC METHODS

To identify which amino acid residues may be responsible for determining acyl-CoA specificity in the carnitine acyltransferase family, bioinformatics methods were used to analyse residues conserved in subfamilies.

5.1. SUBFAMILY CONSERVED RESIDUE ANALYSIS (TREE DETERMINANTS)

Conserved differences between enzymes that catalyse short-chain acyl-CoAs (CrAT and ChAT), medium-chain acyl-CoAs (COT), and long-chain acyl-CoAs (CPTs) were analysed with the SequenceSpace algorithm using a multiple sequence alignment of the carnitine/choline acyltransferase family of proteins as the input (see Appendix). A total of 37 amino acid sequences were considered, including L and M isoforms of CPT I, CPT II, COT, CrAT and ChAT from several organisms.

Seven amino acid residues were identified as putative molecular determinants of acyl-CoA selectivity in the acyltransferase family (Fig. 8). Four of these amino acids were present in all short-chain acyltransferases (CrAT and ChAT) and absent in medium- and long-chain acyltransferases (COT and CPTs, respectively). Thus, the amino acids Ser¹¹⁹, Phe¹³⁸, Gly²⁴⁹ and Ala⁵¹⁵ in rat CrAT coordinates are substituted by Asn¹⁰², Arg¹²⁴, Ala²³⁸ and Gly⁵⁰², respectively, in rat COT.

The remaining three amino acids residues represent conserved differences between COT and CPTs enzymes. Thus, the amino acids Trp⁸⁰, Ser¹⁶⁴ and Leu⁵⁰⁸ in rat COT are substituted by Tyr²³¹, Asn³¹³ and Phe⁶⁵⁸, respectively, in rat L-CPT I.

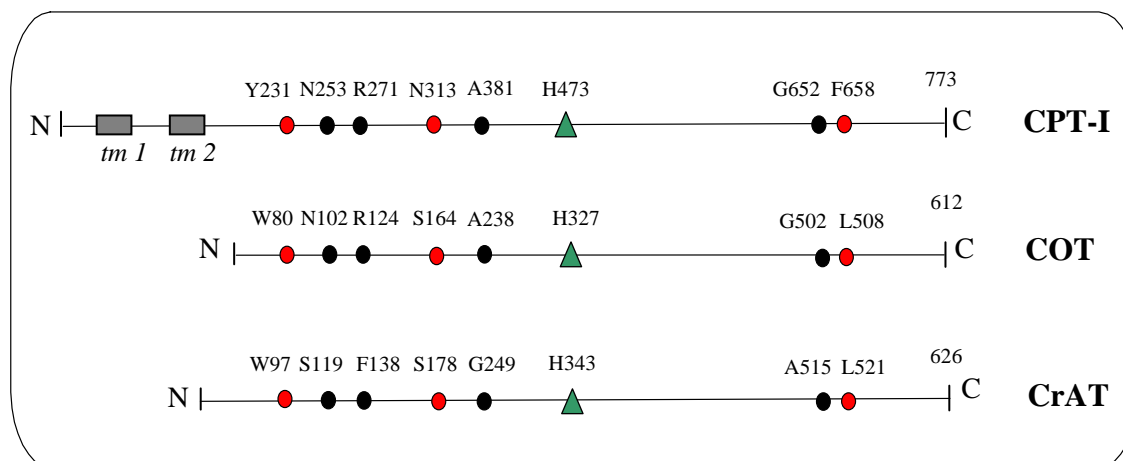


Fig. 8. Schematic representation of the position of the tree-determinant residues obtained using the SequenceSpace algorithm with rat CrAT, COT and L-CPT I proteins. The positions of the conserved differences between CrAT and COT are indicated in black, whereas conserved differences between COT and CPT are indicated in red. The position of the catalytic histidine is indicated in green. The transmembrane regions of L-CPT I are also shown (*tm1* and *tm2*).

5.2. SITE-DIRECTED MUTAGENESIS STUDIES IN RAT CrAT EXPRESSED IN YEAST

To define the role of these amino acids in the acyl-CoA specificity of the carnitine acyltransferase family, we decided to perform a series of site-directed mutagenesis experiments with rat CrAT.

We started by analyzing the four conserved amino acid residue differences between CrAT and COT. To address this issue, we individually replaced Ser¹¹⁹, Phe¹³⁸, Gly²⁴⁹ and Ala⁵¹⁵ in rat CrAT with their counterparts in COT to generate the following CrAT single mutants: S119N, F138R, G249A, and A515G. A mutant that incorporates the four amino substitutions was also prepared (CrAT S119N/F138R/G249A/A515G). The mutants were obtained using a PCR-based mutagenesis procedure (see Materials and Methods, Section 2.14) with the pYESCrAT^{wt} plasmid as template. The following primers were used: CrAT S119N.for and CrAT S119N.rev were used to construct pYESCrAT^{S119N}; CrAT F138R.for and CrAT F138R.rev were used to construct pYESCrAT^{F138R}; CrAT G249A.for and CrAT G249A.rev were used to construct

pYESCrAT^{G249A}; and CrAT A515G.for and CrAT A515G.rev were used to construct pYESCrAT^{A515G}. Finally, pYESCrAT^{S119N/F138R/G249A/A515G} was obtained using the same method, but with the stepwise generation of each new mutation starting from plasmid pYESCrAT^{S119N}. Primer sequences are listed in the Appendix. The appropriate substitutions, as well as the absence of unwanted mutations, were confirmed by sequencing the inserts, as described in Materials and Methods (Section 2.12).

Plasmids containing wild-type CrAT, the point mutants S119N, F138R, G249A, A515G, and the quadruple mutant S119N/F138R/G249A/A515G (QM) were expressed in yeast cells and mitochondrial cell extracts were obtained. Western-blot of yeast-expressed wild-type and mutant proteins showed the same molecular masses and similar expression levels (Fig. 9B). Carnitine acyltransferase activity was measured using acetyl-CoA and decanoyl-CoA as substrates (Fig 9A). Decanoyl-CoA was assayed to assess whether any of the mutants had acquired activity toward medium-chain acyl-CoAs.

The S119N, F138R, and G249A mutations reduced CrAT activity toward its natural substrate acetyl-CoA to about 50% of that of the wild-type enzyme. In the QM, acetyl-CoA activity was almost abolished, showing an activity only 4% of that of the wild-type. Finally, the CrAT mutant A515G showed a modest increase in its activity toward acetyl-CoA.

None of the mutants showed an increase in activity toward the medium-chain substrate decanoyl-CoA when compared to wild-type CrAT (Fig. 9A). Activity toward decanoyl-CoA was almost zero in mutants S119N, G249A and QM, and only the F138R and A515G mutants displayed a similar activity (15 and 20 nmol·min⁻¹·mg protein⁻¹, respectively) to that of the wild-type (20 nmol·min⁻¹·mg protein⁻¹). None of these mutations allowed CrAT to acquire a new activity towards medium-chain acyl-CoAs.

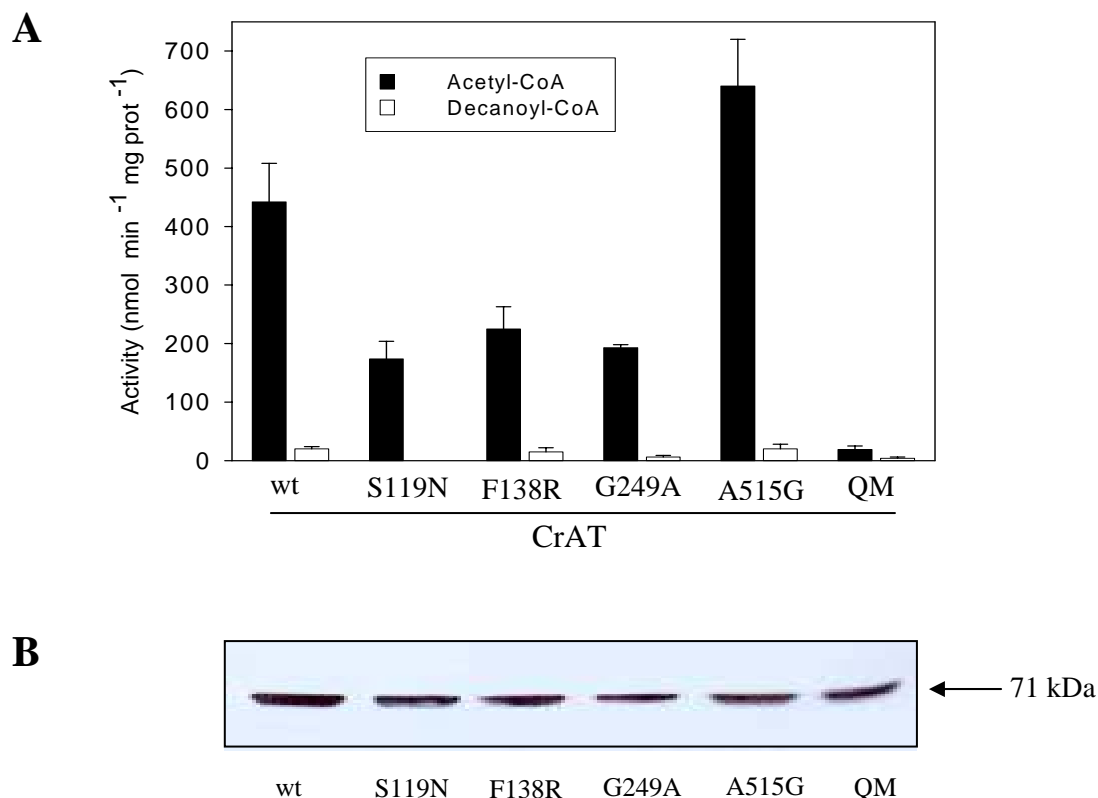


Fig. 9. Carnitine acyltransferase activity in yeast cells expressing wt CrAT, the point mutants S119N, F138R, G249A, and A515G, and the quadruple mutant (QM). A) Mitochondrial protein (5 μ g) from yeast expressing wt CrAT and CrAT mutants S119N, F138R, G249A, A515G, and QM were assayed for activity with acetyl- and decanoyl-CoA. Results are shown as the mean \pm S.D. of three independent experiments. B) Immunoblots showing expression of wt CrAT and mutants S119N, F138R, G249A, A515G, and QM. Yeast samples (8 μ g) were separated by 8% SDS-PAGE and subjected to immunoblotting using specific antibodies. The arrow indicates the migration position and the molecular mass of rat CrAT.

A series of kinetic experiments was performed with CrAT point mutants using acetyl-CoA as the substrate (Table 3). Determination of the kinetic constants for CrAT QM was not possible due to its low activity. All four point mutants had K_m values for acetyl-CoA similar to that of the wild-type enzyme, and therefore, none of the mutations had any effect on the affinity of the enzyme toward the acetyl-CoA substrate. The V_{max} decreased by 60% in the S119N and G249A mutants, and by 45% in the F138R mutant, whereas a slight increase in V_{max} was observed in the A515G mutant. Catalytic efficiency for acetyl-CoA of all four point mutants was very similar to that of the wild-type.

Results

Kinetic parameters for carnitine were also determined using acetyl-CoA as the substrate. The S119N and F138R mutations caused a 2-fold increase in the K_m for carnitine, and the G249A and A515G mutations also produced a slight increase in the K_m for carnitine. Catalytic efficiency was decreased by 3-fold in CrAT mutants S119N, F138R and G249A, whereas no changes in catalytic efficiency were observed in the A515G mutant.

The results suggest that the four mutants have little, if any, effect on substrate selectivity in the CrAT enzyme.

CrAT	K_m		V_{max}		Catalytic efficiency	
	L-carnitine	acetyl-CoA	L-carnitine	acetyl-CoA	L-carnitine	acetyl-CoA
	μM		$\text{nmol}\cdot\text{min}^{-1}\cdot\text{mg protein}^{-1}$		V_{max} / K_m	
Wild-type	203 \pm 21	22.8 \pm 1.0	515 \pm 56	550 \pm 99	2.53	24.1
S119N	425 \pm 64	12.7 \pm 1.6	260 \pm 46	210 \pm 11	0.61	16.6
F138R	451 \pm 52	15.8 \pm 1.5	331 \pm 19	308 \pm 21	0.73	19.5
G249A	320 \pm 4.2	14.4 \pm 3.0	238 \pm 41	207 \pm 34	0.74	14.4
A515G	321 \pm 18	22.8 \pm 4.3	603 \pm 8.0	616 \pm 12	1.88	27.0

Table 3. Kinetic parameters of carnitine acetyltransferase in *S. cerevisiae* cells expressing wt CrAT, and point mutants S119N, F138R, G249A, and A515G. Results are shown as the mean \pm S.D. of at least three independent experiments.

6. STRUCTURE-BASED FUNCTIONAL ANALYSIS OF CrAT

The available 3-D structures of mouse and human carnitine acetyltransferase have provided valuable insights into the study of the molecular determinants of substrate specificity and catalytic activity in the acyltransferase family.

6.1. AMINO ACID RESIDUES INVOLVED IN CATALYSIS

It is generally accepted that a histidine is the main catalytic residue in carnitine acyltransferases. This critical histidine has been mutated in several proteins of the carnitine acyltransferase family, such as rat CPT II, L-CPT I, and COT (Brown, 1994; Morillas, 2001; Morillas, 2000), and in all the cases the mutation completely abolished enzyme activity. The histidine at this position is strictly conserved among members of the acyltransferase family and the homologous residue in rat CrAT is His³⁴³, as was observed in an alignment of representative sequences of mammalian carnitine acyltransferases (Fig. 10). In the human CrAT structure, a glutamate residue (Glu³⁴⁷) interacts with His³⁴³ and appears to be critical for catalysis (Wu, 2003). In almost all the other members of the family, an aspartate is found at this position, which could functionally be substituted for glutamate (Fig. 10).

To define the role of His³⁴³ and Glu³⁴⁷ in the catalytic activity of CrAT, each amino acid was mutated individually to Ala in rat CrAT. The mutations were introduced using a PCR-based mutagenesis procedure with the pYESCrAT^{wt} plasmid as template. CrAT H343A.for and CrAT H343A.rev primers were used to construct pYESCrAT^{H343A}, and CrAT E347A.for and CrAT E347A.rev were used to construct pYESCrAT^{E347A}. Both plasmids were expressed in an *S. cerevisiae* strain lacking endogenous CrAT activity and mitochondrial extracts were obtained. Enzyme activity was abolished in the H343A mutant (Fig. 11A), confirming the key role of His³⁴³ in catalysis. Mutation of Glu³⁴⁷ to Ala also resulted in a total loss of catalytic activity, suggesting that this amino acid also plays an important role in activity (Fig. 11A). Both CrAT mutants were expressed in *S. cerevisiae* at similar levels to the wild-type (Fig. 11B), indicating that abolition of activity was not caused by low protein expression.

Results

CPT1_RAT	469	INAEHSWADAPIVGHLEWYVVMATDVFQ	495
CPT1_MOUSE	460	INAEHSWADAPIVGHLEWYVVMATDVFQ	486
CPT1_HUMAN	469	LNAEHSWADAQIVAHLEWYVMSIDSLQ	495
CPTM_RAT	469	LNTEHSWADAPIIGHLEWYVFLATDTFH	495
CPTM_HUMAN	469	LNAEHAWADAPIIGHLEWYVFLGTDSEH	495
CPT2_RAT	368	VHFEHSWGDGVAVLRFFNEVFRDSTQ	393
CPT2_MOUSE	368	VHFEHAWGDGVAVLRFFNEVFRDSTQ	393
CPT2_HUMAN	368	VHFEHSWGDGVAVLRFFNEVFRDSTQ	393
OCTC_RAT	323	CSCDHAPYDAMLNVNIAHYVDEKLEET	349
OCTC_HUMAN	323	CNCDHAPFDAMIMVNISYYVDEKIFQN	349
OCTC_BOVIN	323	SMCDHAPFDAMVLVKVCYYVDENILEN	349
CACP_HUMAN	339	LVYEHAAAEGFPITVLLDYWIEYTKKP	365
CACP_MOUSE	340	MVYEHAAAEGPPIVALVDHWMEYTKKP	366
CACP_RAT	339	MVYEHAAAEGPPIVALVDHWMEYTKKP	365

6.2. AMINO ACIDS RESIDUES INVOLVED IN ACYL-CoA SPECIFICITY

6.2.1. The M564G mutation causes conversion of CrAT into COT

Inspection of the published crystal structure of CrAT revealed that the acetyl moiety of acetylcarnitine points to a hydrophobic pocket at the intersection of two β -sheets (strands E1 and E8 in the N domain and E13 and E14 in the C domain) and α -helix H12 (Jogl, 2003). This pocket is partly occupied by the side chain of Met⁵⁶⁴ from strand E14. Because this methionine is only present in CrAT and not in other carnitine acyltransferases (CPT I, CPT II and COT), in which the equivalent residue is a glycine (Fig. 12), we hypothesized that it could play a role in the correct positioning of the hydrocarbon chain of acyl-CoA. Therefore, we prepared the CrAT mutant M564G, which was then expressed in yeast. The mutation was introduced using a PCR-based mutagenesis procedure with the pYESCrAT^{wt} plasmid as template and using the primers CrAT M564G.for and CrAT M564G.rev.

		E13		E14	
		EEEEEEE		EEE	
CPT1_RAT	683	RLSTSQT	PQQQVELFD	FEKNPDYV	SCGGGFGPVA 716
CPT1_MOUSE	674	RLSTSQT	PQQQVELFD	FEKYPDYV	SCGGGFGPVA 707
CPT1_HUMAN	683	RLSTSQT	PQQQVELFD	LENNPEYV	SSGGGFGPVA 716
CPTM_RAT	683	SLSTSQI	PQFQICMFD	PKQYPNHL	GAGGGFGPVA 716
CPTM_HUMAN	683	RLSTSQI	PQSQIRMFD	PEQHPNHL	GAGGGFGPVA 716
CPT2_RAT	586	ILSTSTLN	SPAVSLGG	FAPVV 606
CPT2_MOUSE	586	ILSTSTLS	SPAVSLGG	FAPVV 606
CPT2_HUMAN	586	VLSTSTLS	SPAVNLGG	FAPVV 606
OCTC_RAT	540	VLSTSLVG	YLRICGVV	VPMV 559
OCTC_HUMAN	540	VLSTSLVG	YLRVQGVV	VPMV 559
OCTC_BOVIN	540	VLSTSLVG	YLRVQGVV	VPMV 559
CACP_HUMAN	550	HLSTSQVP	AKTDCVMF	FGPVV 570
CACP_MOUSE	551	NLSTSQVP	AKTDCVMF	FGPVV 571
CACP_RAT	550	NLSTSQVP	AKTDCVMS	FGPVV 570

↑
M564

Fig. 12. **Alignment of representative sequences of mammalian carnitine acyltransferases.** Amino acid sequence of carnitine acyltransferase enzymes CrAT (CACP) from human, mouse and rat, L-CPT I (CPT1) from rat, mouse and human, M-CPT I (CPTM) from human, and rat, CPT II (CPT2) from rat, mouse and human, and COT (OCTC) from human, rat and cattle were aligned using ClustalW. Residues are colored according to conservation. The position of the conserved residue according to acyl-chain length specificity (a methionine, Met⁵⁶⁴, for CrAT and a glycine for COT and CPTs) is also noted. The secondary structure elements β -strands E13 and E14 are indicated.

Results

Enzyme activity of the yeast-expressed CrAT mutant M564G was tested for acyl-CoA substrates of various lengths and compared with wild-type CrAT. Wild-type CrAT was highly active toward acetyl- and butyryl-CoA but not toward longer acyl-CoAs (Fig. 13A). In contrast, CrAT mutant M564G (Fig. 13B) was more active toward longer acyl-CoAs: it showed a new activity toward palmitoyl-CoA and a 1250-fold increase in activity toward myristoyl-CoA (Table 4). This figure was calculated after determination of enzyme activities with highly purified wt CrAT after expression in *E. coli*, since activity with myristoyl-CoA was undetectable in the mitochondrial fraction from yeast expressing wt CrAT. Activity also increased with dodecanoyl- (58-fold), decanoyl- (7-fold), octanoyl- (11-fold), and hexanoyl-CoA (6-fold), while activity toward acetyl-CoA decreased by 50% (Table 4). Surprisingly, CrAT mutant M564G was very active with myristoyl-CoA, but much less so with palmitoyl-CoA (409 and 18.0 nmol·min⁻¹·mg protein⁻¹, respectively). These values indicate that the long side chain of methionine impedes the positioning of medium- and long-chain acyl-CoAs in the hydrophobic pocket, but when this side chain is shortened (as in the mutant), other, longer acyl-CoAs fit in the fatty acid binding site and catalysis proceeds. Mutation of Met⁵⁶⁴ to Gly creates an artificial enzyme that behaves like COT in terms of acyl-CoA specificity (Fig 13B and D).

	Activity			Variation (fold)	
	wt	M564G	M564A	M564G	M564A
	nmol·min ⁻¹ ·mg protein ⁻¹				
C ₂ -CoA	442 ± 66	234 ± 30	234 ± 12	(x 0.5)	(x 0.5)
C ₄ -CoA	553 ± 62	641 ± 3.2	557 ± 40	(x 1.2)	(x 1)
C ₆ -CoA	119 ± 16	802 ± 66	532 ± 50	(x 6)	(x 5)
C ₈ -CoA	45.7 ± 6.5	488 ± 24	239 ± 34	(x 11)	(x 5)
C ₁₀ -CoA	20.3 ± 4.1	136 ± 7.3	81.9 ± 6.5	(x 7)	(x 4)
C ₁₂ -CoA	6.0 ± 2.6	350 ± 5.0	136 ± 22	(x 58)	(x 23)
C ₁₄ -CoA	0.33 ± 0.07 ^a	409 ± 29	80 ± 14	(x 1250)	(x 242)
C ₁₆ -CoA	0	18.0 ± 3.6	10.7 ± 5.2		

Table 4. **Enzyme activity of wild-type CrAT and M564G and M564A mutants expressed in *S. cerevisiae*.** Mitochondrial protein from yeast expressing wt CrAT and M564G and M564A mutants were assayed with acyl-CoAs of different carbon-chain lengths ranging from acetyl- to palmitoyl-CoA. Results are shown as the mean ± S.D. of three independent experiments. The fold variation in activity compared with the wild-type is shown in parentheses. ^a Activity obtained using purified rat CrAT.

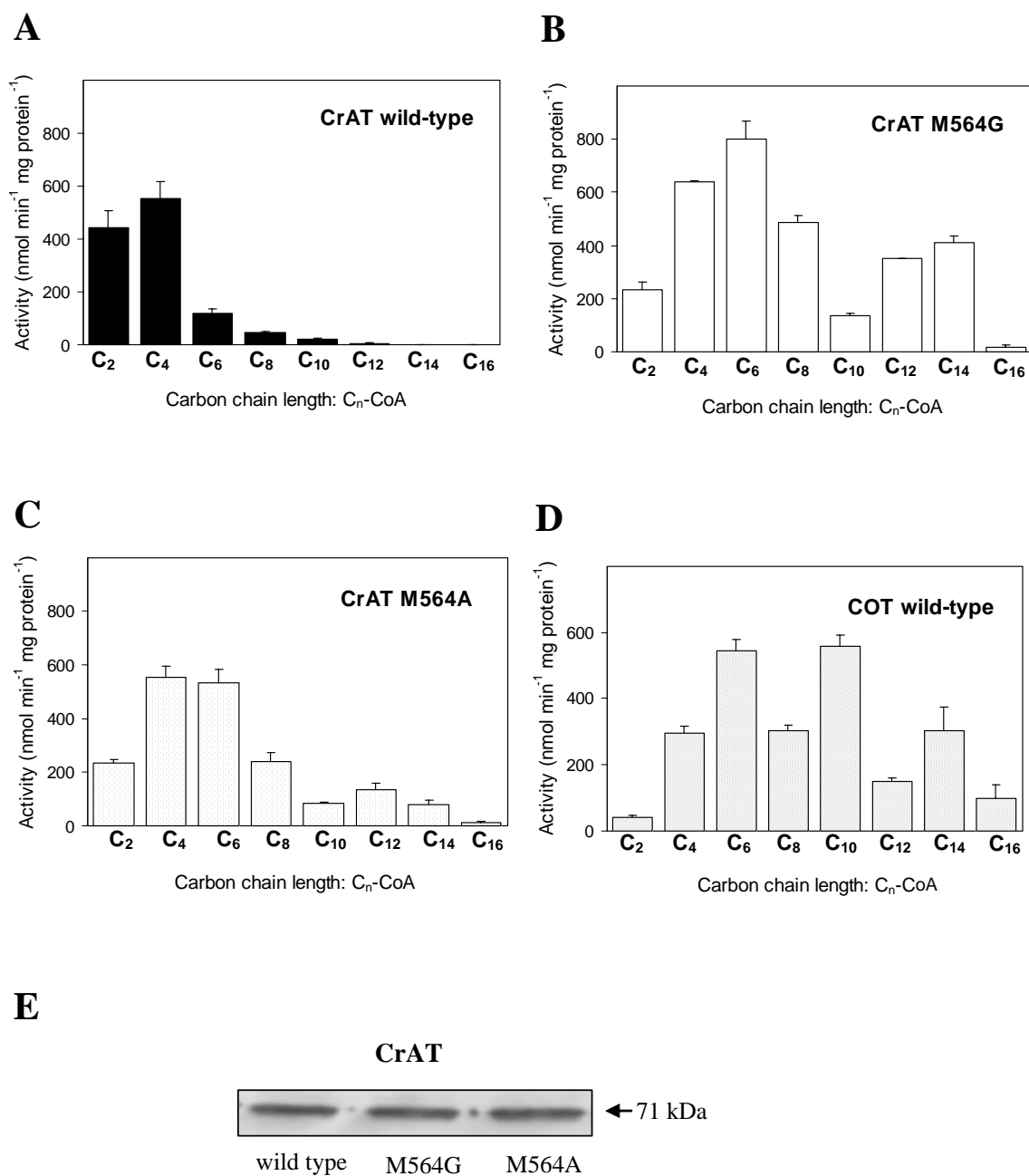


Fig. 13. Carnitine acyltransferase activity of *S. cerevisiae* cells expressing wt CrAT and COT, and the point mutants CrAT M564G and M564A. Extracts from yeast expressing wt CrAT (A), wt COT (D), and point mutants CrAT M564G (B) and M564A (C) were assayed for activity with acyl-CoAs of different chain length ranging from acetyl-CoA to palmitoyl-CoA. Results are shown as the mean \pm S.D. of at least three independent experiments. Immunoblots showing expression of wt CrAT, CrAT M564G and M564A (E). *S. cerevisiae* extracts (8 μ g) were separated by SDS-PAGE and subjected to immunoblotting using specific antibodies. The arrows indicate the migration position and the molecular mass of rat CrAT.

6.2.2. Kinetic characteristics of CrAT mutant M564G

A series of kinetic experiments was performed with CrAT mutant M564G by varying the length of the acyl-CoA substrate from C₂- to C₁₄-CoA (Table 5). The mutant showed standard saturation kinetics for both carnitine and acyl-CoA substrates (Fig. 14). This property was general for all acyl-CoAs, irrespective of their length.

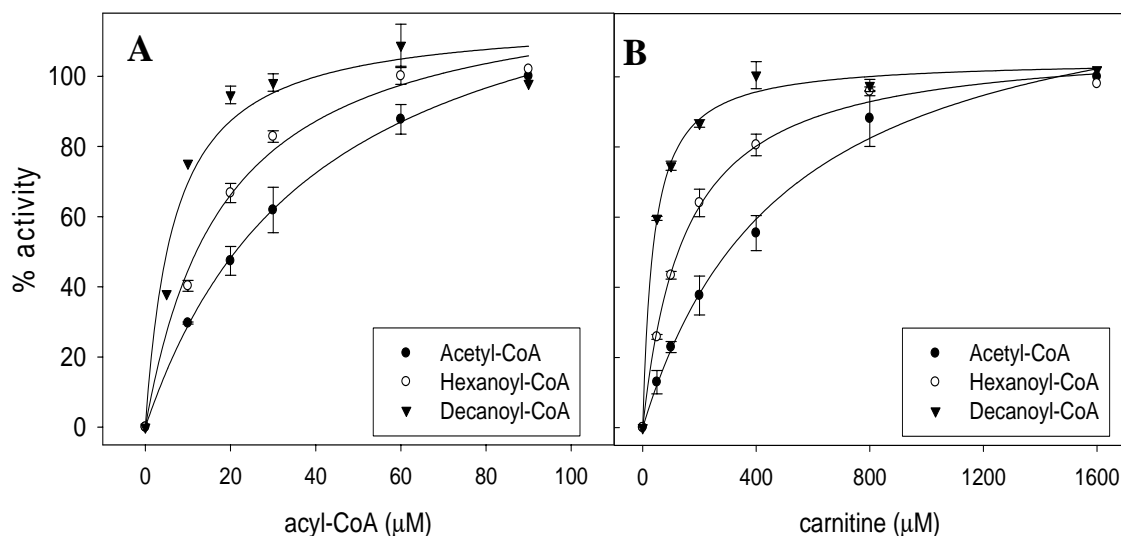


Fig. 14. **Carnitine and acyl-CoA saturation curves for CrAT M564G expressed in yeast.** Mitochondrial protein (5 μg) from yeast expressing CrAT was assayed for carnitine acyltransferase activity either at 1500 μM carnitine with increasing concentrations of acyl-CoA (A) or at 100 μM acyl-CoA with increasing concentrations of carnitine (B). Results are shown as the mean ± S.D. of three independent experiments.

Although K_m values for fatty acyl-CoA varied slightly with the chain length (between 11 and 32 μM), V_{max} increased, particularly with hexanoyl-CoA (1120 nmol·min⁻¹·mg protein⁻¹) (Table 5). Another activity maximum was observed with myristoyl-CoA. The K_m for carnitine decreased when the acyl-CoA was long, showing that the mutant preferred long-chain acyl-CoAs as substrates. Catalytic efficiencies for both carnitine and acyl-CoA increased with the length of acyl-CoA, values for hexanoyl-CoA and octanoyl-CoA being the highest. In contrast to the wt CrAT, mutant M564G behaved as if its natural substrates were medium- and long-chain acyl-CoAs. These results were interpreted as showing that replacement of methionine with glycine increased the space for positioning of carnitine and acyl-CoA and that this in turn produces an increase in its catalytic efficiency for longer acyl-CoAs.

Results

	K_m		V_{max}		Catalytic efficiency	
	Carnitine	Acyl-CoA	Carnitine	Acyl-CoA	Carnitine	Acyl-CoA
	μM		$\text{nmol}\cdot\text{min}^{-1}\cdot\text{mg protein}^{-1}$		V_{max}/K_m	
C ₂ -CoA	339 ± 44	31.7 ± 5.3	197 ± 20.8	243 ± 25	0.58	7.7
C ₄ -CoA	170 ± 45	14.8 ± 1.0	742 ± 133	872 ± 125	4.4	59
C ₆ -CoA	164 ± 11	22.3 ± 6.0	1145 ± 255	1120 ± 106	7.0	50
C ₈ -CoA	86.0 ± 6.1	10.9 ± 3.6	522 ± 106	653 ± 110	6.1	60
C ₁₀ -CoA	26.9 ± 6.9	10.8 ± 1.7	153 ± 10.6	257 ± 41.6	5.7	24
C ₁₄ -CoA	309 ± 50	12.7 ± 2.5	562 ± 84.6	505 ± 83.5	1.9	40

Table 5. **Kinetic parameters of the CrAT mutant M564G in yeast.** Mitochondrial protein from yeast expressing the CrAT mutant M564G was assayed with acyl-CoAs of different carbon-chain lengths, ranging from C₂- to C₁₄-CoA. Results are shown as the mean ± S.D. of three independent experiments.

6.2.3. The M564A mutation also broadens the specificity of CrAT

Because glycine does not constrain the backbone psi/phi angles, its substitution for methionine could modify substrate specificity simply as a result of increased flexibility. To rule out this possibility, we prepared another CrAT mutant, M564A. Alanine is also a small amino acid, but unlike glycine, it does not affect flexibility. Thus, if methionine/glycine acts as a molecular gate to prevent/permit acyl-CoA binding as a function of chain-length, the alanine mutant should behave similarly to the glycine mutant. The change in specificity of the alanine mutant might not be as pronounced, but it would still be able to catalyse acyl-CoAs longer than acetyl- and butyryl-CoA. Accordingly, we expressed the CrAT mutant M564A in yeast and assayed the extracts for activity using acyl-CoAs of various chain lengths as substrates. The results were similar to those found with the M564G mutant (Table 4 and Fig. 13C). The activity of the CrAT mutant M564A toward myristoyl-CoA increased 242-fold with respect to the wt CrAT. The M564A mutant displayed a 5- to 23-fold activation with acyl-CoAs of between C₆ and C₁₂. Unlike wt CrAT, mutant M564A also showed some activity toward

palmitoyl-CoA (11 nmol·min⁻¹·mg protein⁻¹). In addition, the activity of CrAT mutant M564A toward its natural substrate acetyl-CoA was less than half that of wt CrAT.

6.2.4. Role of the cluster ⁵⁶³VMS⁵⁶⁵ in acyl-CoA specificity

Our biochemical studies show that the Met⁵⁶⁴ residue has an important role in determining the substrate preference of CrAT. Met⁵⁶⁴ is part of a cluster of three residues, ⁵⁶³VMS⁵⁶⁵ in rat CrAT, that are replaced by three glycines in CPT I, as observed in the sequence alignment (Fig. 15). These residues are located in strand E14, which helps enclose the acyl group binding site. To define the role of this cluster of residues in the enzyme-acyl-CoA specificity, we prepared the CrAT triple mutant V563G/M564G/S565G (CrAT mutant GGG). The mutations were introduced using a PCR-based mutagenesis procedure with the pYESCrAT^{M564G} plasmid as template and using primers CrAT GGG.for and CrAT GGG.rev. The triple mutant was then expressed in yeast.

		E13		E14						
		EEEEEEE		EEE						
CPT1_RAT	683	RLSTS	QTPQQQVELFD	FEK	NP	DYV	SC	GGCF	GPVA	716
CPT1_MOUSE	674	RLSTS	QTPQQQVELFD	FEK	YP	DPY	VS	CGCF	GPVA	707
CPT1_HUMAN	683	RLSTS	QTPQQQVELFD	LENN	PEY	VSS	GGCF	GPVA	716	
CPTM_RAT	683	SLSTS	QIPQFQICM	FDP	KQY	PNHL	GAG	CGF	GPVA	716
CPTM_HUMAN	683	RLSTS	QIPQSQIRM	FDP	EQH	PNHL	GAG	CGF	GPVA	716
CPT2_RAT	586	ILSTSTLN	SPAV	SL	CGF	APV	V	606	
CPT2_MOUSE	586	ILSTSTLS	SPAV	SL	CGF	APV	V	606	
CPT2_HUMAN	586	VLSTSTLS	SPAV	NL	CGF	APV	V	606	
OCTC_RAT	540	VLSTSLVG	YLR	IQ	VV	VP	MP	559	
OCTC_HUMAN	540	VLSTSLVG	YLR	VQ	VV	VP	MP	559	
OCTC_BOVIN	540	VLSTSLVG	YLR	VQ	V	VP	MP	559	
CACP_HUMAN	550	HLSTS	QVP	AKT	DQ	VM	FF	GPV	570
CACP_MOUSE	551	NLSTS	QVP	AKT	DQ	VM	FF	GPV	571
CACP_RAT	550	NLSTS	QVP	AKT	DQ	VM	SF	GPV	570

Fig. 15. Alignment of representative sequences of mammalian carnitine acyltransferases. Amino acid sequences of carnitine acyltransferase enzymes CrAT (CACP) from human, mouse and rat, L-CPT I (CPT1) from rat, mouse and human, M-CPT I (CPTM) from human and rat, CPT II (CPT2) from rat, mouse and human, and COT (OCTC) from human, rat and cattle were aligned using ClustalW. Residues are colored according to conservation. The cluster of three residues (⁵⁶³VMS/^{F565} for CrAT and ⁷⁰⁹GGG⁷¹¹ for CPT I) is enclosed by a box. Secondary structure elements are indicated.

Enzyme activity of the yeast-expressed CrAT triple mutant GGG was tested for acyl-CoA substrates of various lengths from acetyl- to palmitoyl-CoA and compared with the CrAT mutant M564G (Fig. 16A). As described in Section 6.2.1, the CrAT mutant M564G exhibited high activity toward medium-chain acyl-CoAs, especially hexanoyl- and myristoyl-CoA (802 and 409 nmol·min⁻¹·mg protein⁻¹, respectively). The GGG mutant also showed high activity with medium-chain acyl-CoAs (Table 6). The activity with hexanoyl-CoA was 273 nmol·min⁻¹·mg protein⁻¹, and maximum activity was observed with myristoyl-CoA (302 nmol·min⁻¹·mg protein⁻¹). The GGG mutant showed a 4-fold increase in activity toward palmitoyl-CoA when compared with the single mutant M564G. Interestingly, the GGG mutant showed diminished activity toward short-chain acyl-CoAs. Activity toward C₂- and C₄-CoA was only 22.7 and 38.1 nmol·min⁻¹·mg protein⁻¹, respectively. In contrast the M564G mutant still displayed high activity toward C₂- and C₄-CoA (234 and 641 nmol·min⁻¹·mg protein⁻¹, respectively).

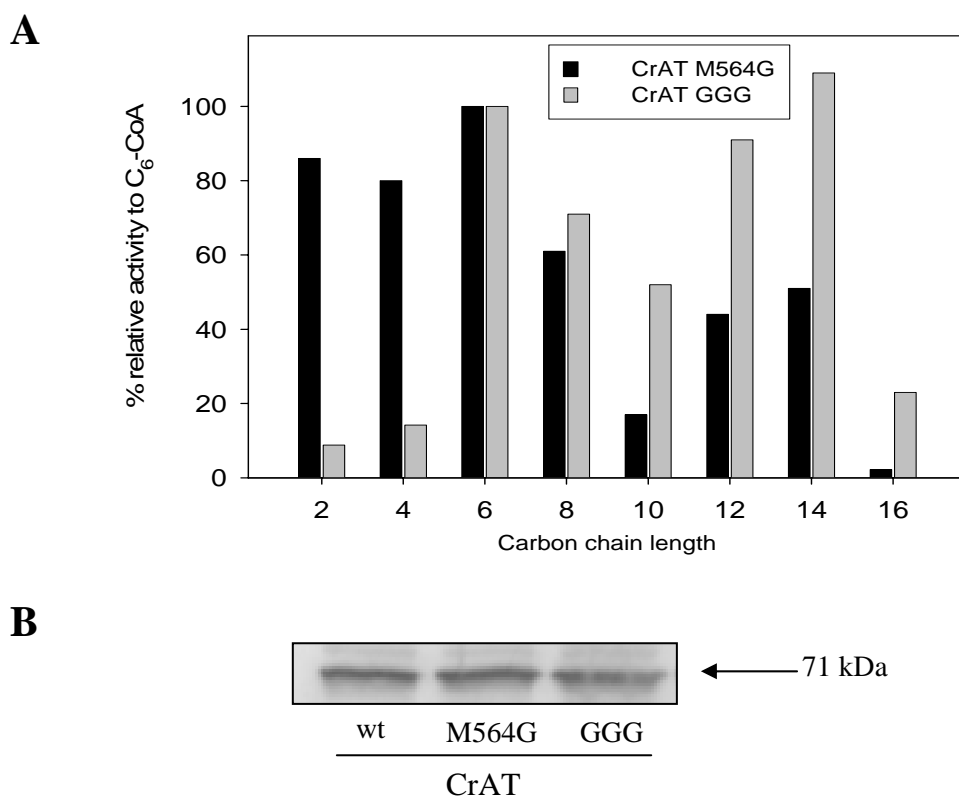


Fig. 16. Carnitine acetyltransferase activity of *S. cerevisiae* cells expressing CrAT mutant M564G and CrAT mutant V563G/M564G/S565G (GGG). A) Mitochondrial protein from yeast expressing CrAT mutants M564G and GGG were assayed for activity with acyl-CoAs of different carbon-chain lengths ranging from C₂- to C₁₆-CoA. The results are expressed as the relative acyl-CoA activity compared to hexanoyl-CoA (scaled to 100). B) *S. cerevisiae* extracts (8 μg) were separated by SDS-PAGE and subjected to immunoblotting. The arrows indicate the migration position and the molecular mass of rat CrAT.

A series of kinetic experiments was performed by varying the length of the acyl-CoA substrate from hexanoyl- to myristoyl-CoA (Table 6). The GGG mutant showed standard saturation kinetics for both carnitine and acyl-CoA substrates (Fig. 17). This property was general for all acyl-CoAs, irrespective of their length (data not shown).

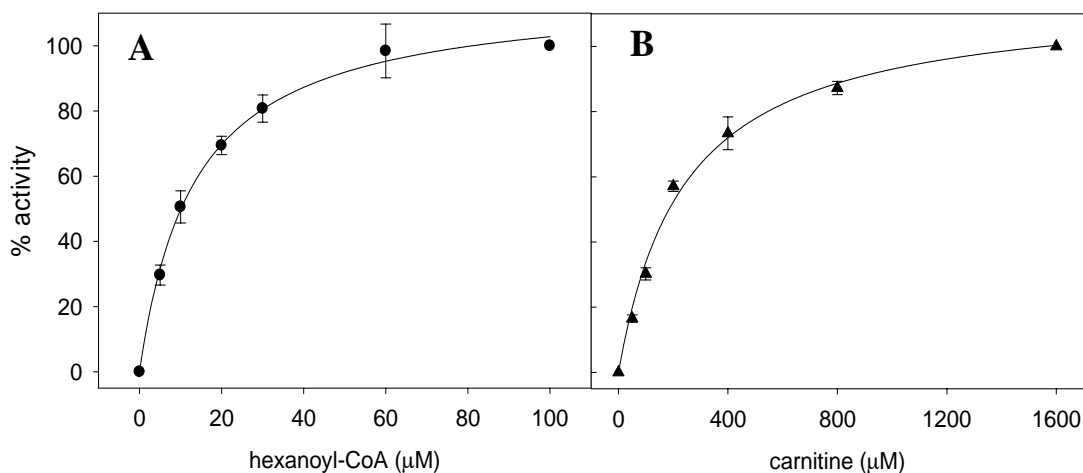


Fig. 17. **Carnitine and hexanoyl-CoA saturation curves for the CrAT triple mutant V563G/M564G/S565G (GGG) expressed in yeast.** Mitochondrial protein (5 μg) from yeast expressing the CrAT mutant GGG was assayed for carnitine acyltransferase activity either at 1500 μM carnitine with increasing concentrations of hexanoyl-CoA (A) or at 100 μM hexanoyl-CoA with increasing concentrations of carnitine (B). Results are shown as the mean ± S.D. of three independent experiments.

K_m values for fatty acyl-CoA varied slightly (between 6 and 10 μM) with the carbon-chain length, and V_{max} was maximal for hexanoyl- and myristoyl-CoA. Catalytic efficiency was maximal for myristoyl-CoA, unlike in the CrAT mutant M564G, which showed maximal catalytic efficiency values with hexanoyl- and octanoyl-CoA (Table 6). The K_m for carnitine of the GGG mutant decreased with the chain length of the acyl-CoA substrate, as observed with the M564G mutant. The K_m for carnitine with decanoyl-CoA as substrate was 5-fold lower than that of hexanoyl-CoA (55 and 263 μM, respectively), showing that the CrAT triple mutant preferred medium-chain acyl-CoAs as substrates. Western-blot of wt CrAT and CrAT mutants M564G and GGG expressed in yeast showed the same molecular mass and similar expression levels (Fig. 16B). These results show that the replacement of a cluster of three residues in rat CrAT ($^{563}\text{VMS}^{565}$) with the orthologous amino acids in CPTs (three glycines) increases the space for positioning of carnitine and acyl-CoA in the active site and that this in turn produces an increase in its catalytic efficiency for longer acyl-CoAs.

Results

Acyl-CoA	Activity	K_m		V_{max}		Catalytic efficiency	
		Carnitine	Acyl-CoA	Carnitine	Acyl-CoA	Carnitine	Acyl-CoA
	nmol·min ⁻¹ ·mg ⁻¹	μM		nmol·min ⁻¹ ·mg ⁻¹		V_{max}/K_m	
C ₂ -CoA	22.7 ± 9.9	-	-	-	-	-	-
C ₄ -CoA	38.1 ± 13	-	-	-	-	-	-
C ₆ -CoA	273 ± 49	263 ± 2.0	10 ± 0.8	375 ± 28	303 ± 33	1.4	30.3
C ₈ -CoA	196 ± 33	175 ± 22	5.7 ± 1.6	220 ± 21	194 ± 37	1.3	34.0
C ₁₀ -CoA	142 ± 21	55 ± 14	8.5 ± 2.7	178 ± 18	180 ± 21	3.2	21.1
C ₁₂ -CoA	250 ± 33	-	-	-	-	-	-
C ₁₄ -CoA	302 ± 20	-	6.3 ± 1.0	-	303 ± 43	-	52.4
C ₁₆ -CoA	65.1 ± 19	-	-	-	-	-	-

Table 6. **Enzyme activity and kinetic parameters of CrAT mutant V563G/M564G/S565G (GGG) in *S. cerevisiae*.** Mitochondrial protein (5 μg) from yeast expressing the CrAT mutant GGG was assayed with acyl-CoAs of different carbon-chain lengths, ranging from acetyl- to palmitoyl-CoA. Results are shown as the mean ± S.D. of three independent experiments.

6.2.5. Re-engineering COT acyl-CoA specificity

Through the experiments performed above (Section 6.2.1.), we converted rat CrAT into pseudo rat COT by mutating a single amino acid residue (CrAT Met⁵⁶⁴). Our aim was then to achieve the opposite, that is, to transform rat COT into a pseudo rat CrAT by modifying a single amino acid. We decided to mutate COT Gly⁵⁵³ (orthologous to CrAT Met⁵⁶⁴) to methionine. The mutation was introduced by PCR using the primers COT G553M.for and COT G553M.rev and the pYESCOT^{wt} plasmid as template, resulting in the pYESCOT^{G553M} construct.

Enzyme activity of the COT mutant G553M expressed in yeast was tested with substrates of different length and compared with wt COT (Table 7 and Fig. 18A and B). The G553M mutant showed much lower activity toward medium- and long-chain acyl-CoAs than the wt enzyme, but a slight increase in activity toward short-chain acyl-CoAs (acetyl- and butyryl-CoA), showing maximum activity toward butyryl-CoA, unlike wt

COT, but similar to wt CrAT (Fig 18). The G553M mutant showed a 31-fold reduction in activity compared with wt COT when octanoyl-CoA was the substrate. Activity with hexanoyl-CoA also decreased (9 fold). The activity of the G553M mutant toward acyl-CoAs with chains containing between 10 and 16 carbons was undetectable, making the profile of activities toward the whole list of acyl-CoAs practically identical to that of wt CrAT. Mutation of Gly⁵⁵³ to Met in COT reproduced the substrate specificity of wt CrAT. Western-blot of yeast-expressed wt COT and the G553M mutant showed the same molecular mass and similar expression levels (Fig. 18D).

Acyl-CoA	Activity		Variation fold
	COT wt	COT G553M	
	nmol·min ⁻¹ ·mg protein ⁻¹		
C ₂ -CoA	41.7 ± 7.3	113 ± 7.2	(x 2.7)
C ₃ -CoA	154 ± 14	258 ± 20	(x 1.7)
C ₄ -CoA	297 ± 18	453 ± 60	(x 1.5)
C ₆ -CoA	544 ± 33	70.8 ± 3.1	(x 0.13)
C ₈ -CoA	313 ± 8.2	9.7 ± 0.5	(x 0.03)
C ₁₀ -CoA	540 ± 33	0	-
C ₁₂ -CoA	148 ± 11	0	-
C ₁₄ -CoA	267 ± 27	0	-
C ₁₆ -CoA	77.0 ± 14	0	-

Table 7. **Enzyme activity of wild-type COT and the COT mutant G553M expressed in *S. cerevisiae*.** Results are shown as the mean ± S.D. of at least three independent experiments. The fold variation in activity compared with the wild-type is shown in parentheses.

Kinetic parameters for the G553M mutant were determined using acetyl- and butyryl-CoA as substrates (Table 8). Both K_m and catalytic efficiency values were very similar to those of wt COT. K_m values for acetyl-CoA were 13.0 and 14.6 μ M for wt COT and the G553M mutant, respectively. K_m values for butyryl-CoA were 8.9 and 14.0 μ M for wt COT and the G553M mutant, respectively.

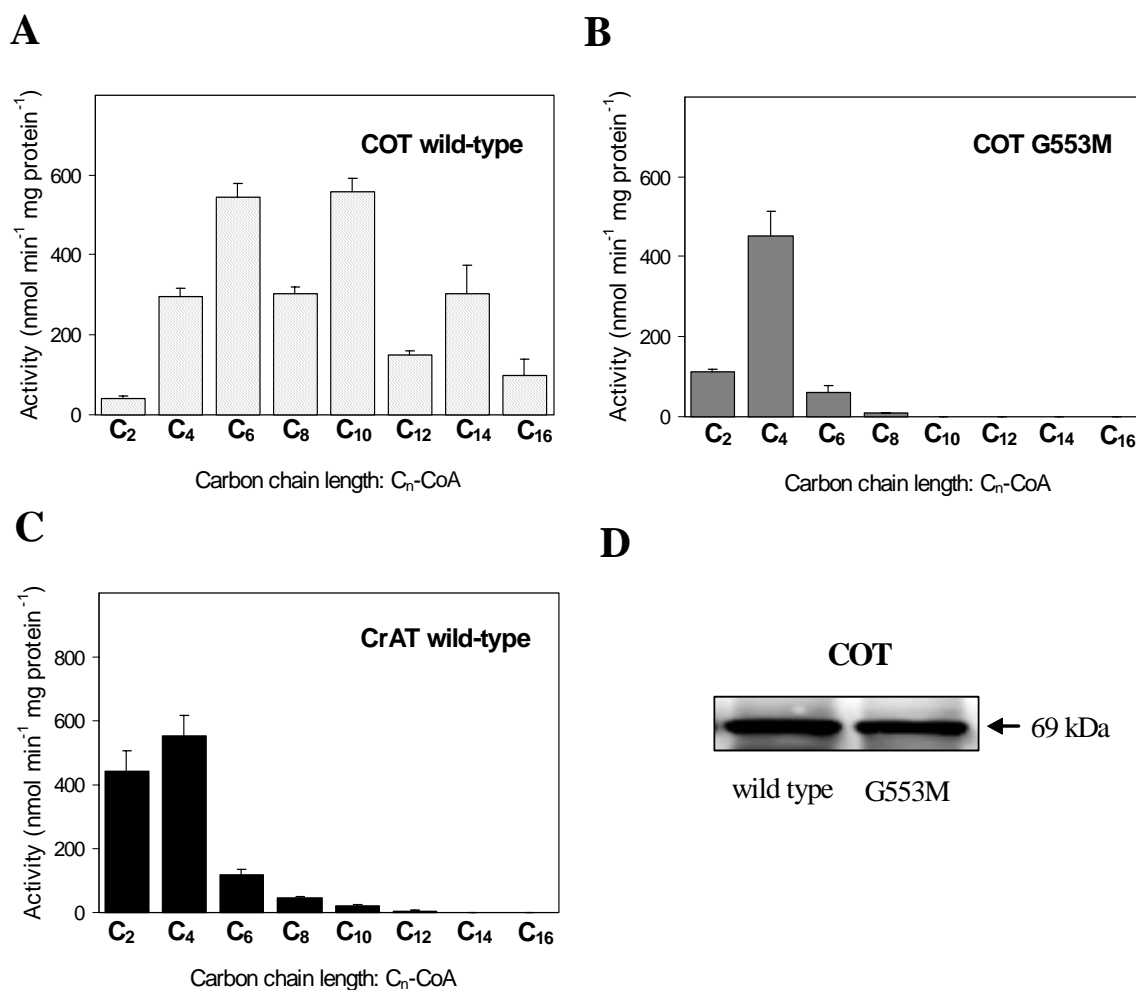


Fig. 18. **Carnitine acyltransferase activity of *S. cerevisiae* cells expressing wt CrAT, wt COT and COT mutant G553M.** Protein extracts from yeast expressing wt COT (A), wt CrAT (C) and COT mutant G553M (B) were assayed for activity with acyl-CoAs of different carbon-chain lengths, ranging from acetyl- to palmitoyl-CoA. Immunoblots showing expression of wt COT and COT G553M (D). *S. cerevisiae* extracts (10 µg) were separated by SDS-PAGE and subjected to immunoblotting using specific antibodies. The arrow indicates the migration position and the molecular mass of rat COT.

Acyl-CoA	K_m (µM)	V_{max} (nmol·min ⁻¹ ·mg protein ⁻¹)	Catalytic efficiency (V_{max}/K_m)
C ₂ -CoA	14.6 ± 0.3	88 ± 14	6.,1
C ₄ -CoA	14.0 ± 3.0	460 ± 95	32.8

Table 8. **Kinetic parameters of rat COT mutant G553M expressed in *S. cerevisiae*.** Protein extracts from yeast expressing the COT mutant G553M were assayed with acetyl-CoA and butyryl-CoA. Results are shown as the mean ± S.D. of at least three independent experiments.

7. MODELS FOR THE POSITIONING OF FATTY ACIDS BASED ON THE CrAT CRYSTAL

7.1. CONSTRUCTION OF THE RAT CrAT AND COT MODELS

To confirm our experimental results, which showed that Met⁵⁶⁴ in CrAT and Gly⁵⁵³ in COT play pivotal roles in determining the acyl-CoA preference of the two enzymes, a model for the location of fatty acyl-CoAs in the active site of both CrAT and COT enzymes was proposed.

Structural models of the rat wt CrAT and COT were generated by homology-modeling procedures using the crystal structures of mouse and human CrAT as templates (Jogl, 2003; Wu, 2003), as described in Materials and Methods (Section 8.4). The 3-D models for the CrAT M564G and COT G553M mutants were built using the structural models of their respective wt enzymes as templates. The carnitine molecule and the CoA part of the acyl-CoAs were located using the information available in the crystal structure of mouse CrAT (Jogl, 2003). Positioning of the acyl part of the acetyl-, decanoyl-, and myristoyl-CoA substrates was modelled using the simulation docking algorithms Autodock and Hex (Materials and Methods, Section 8.5).

7.2. POSITIONING OF THE ACYL-CoA MOLECULE IN THE MODELS

The location of acetyl-CoA in the active site of the model for rat wt CrAT (Fig. 19A) is, as expected, very similar to that described for CoA in the crystallized mouse CrAT. The sulphur atom of the CoA molecule is close to carnitine and to the catalytic His³⁴³, whereas the acetyl group appears to lie in a small cavity defined by the β -sheets E1, E13 and E14 as the walls of the hollow and by the side chain of residue Met⁵⁶⁴ as the floor. Surprisingly, the shape of the cavity appears to be very different in the structure of the active site of the CrAT mutant M564G (Fig. 19B). The small size of the side chain of Gly⁵⁶⁴ reveals a deeper pocket in the same position as the shallow cavity in the wt molecule. This preformed pocket is now accessible to longer acyl groups, as can be modelled using myristoyl-CoA as substrate. The open cavity of CrAT mutant

M564G is surrounded by Gly⁵⁶⁴, by hydrophobic residues Val¹²², Leu¹²⁴, Ile³⁵¹, Val³⁵², Val³⁵⁵, Met³⁵⁹, Val⁵⁵⁶, Ala⁵⁵⁸ and Cys⁵⁶² (located in β -sheets E1, E13 and E14 and in α -helix H12) and by polar residues Asp³⁵⁶ and Thr⁵⁶⁰ at the bottom. Interestingly, it appears that the cavity for longer acyl groups is preformed in CrAT and that Met⁵⁶⁴ acts as a lid to close the access to the hydrophobic pocket (Fig. 20A). When the side chain of Met⁵⁶⁴ is removed, the pocket is now accessible, extending the sensitivity of the enzyme to long-chain acyl-CoA substrates (Fig. 20B). This is consistent with the enzymatic activity observed when using C₈-, C₁₀-, C₁₂- and C₁₄-CoA as substrates (Fig. 18B).

The model for wt COT and its interaction with decanoyl-CoA is very similar to the one for CrAT mutant M564G and myristoyl-CoA. The sulphur atom of the acyl-CoA molecule is close to carnitine and to His³²⁷, the catalytic residue, whereas the fatty acid extension is enclosed in a pocket defined by the side chain of hydrophobic residues positioned in β -sheets E1, E13 and E14 and in α -helix H12: Val¹⁰⁴, Ala³³², Met³³³, Met³³⁵, Val³³⁶, Ala³³⁹, Leu⁵⁴⁵, Leu⁵⁴⁹ and Ile⁵⁵¹ (Fig. 19C). The floor of the cavity is occupied by polar residues Ser¹⁰⁷ and Asp³⁴³. In contrast, the structure for COT mutant G553M resembles that for wt CrAT: the side chain of Met⁵⁵³ now closes the entrance to the pocket and defines a narrow cavity, structurally equivalent to that of the active centre in wt CrAT, where the small acetyl group of acetyl-CoA can be fitted (Fig. 19D). In symmetry with CrAT, the hydrophobic cavity for long acyl-CoAs in the COT structure can be closed by the lateral chain of Met⁵⁵³, which acts as a lid, like the corresponding residue in CrAT, Met⁵⁶⁴. The model again correlates with the enzymatic activities of wt and mutant COT when using short- and long-chain acyl-CoAs as substrates (Fig. 18).

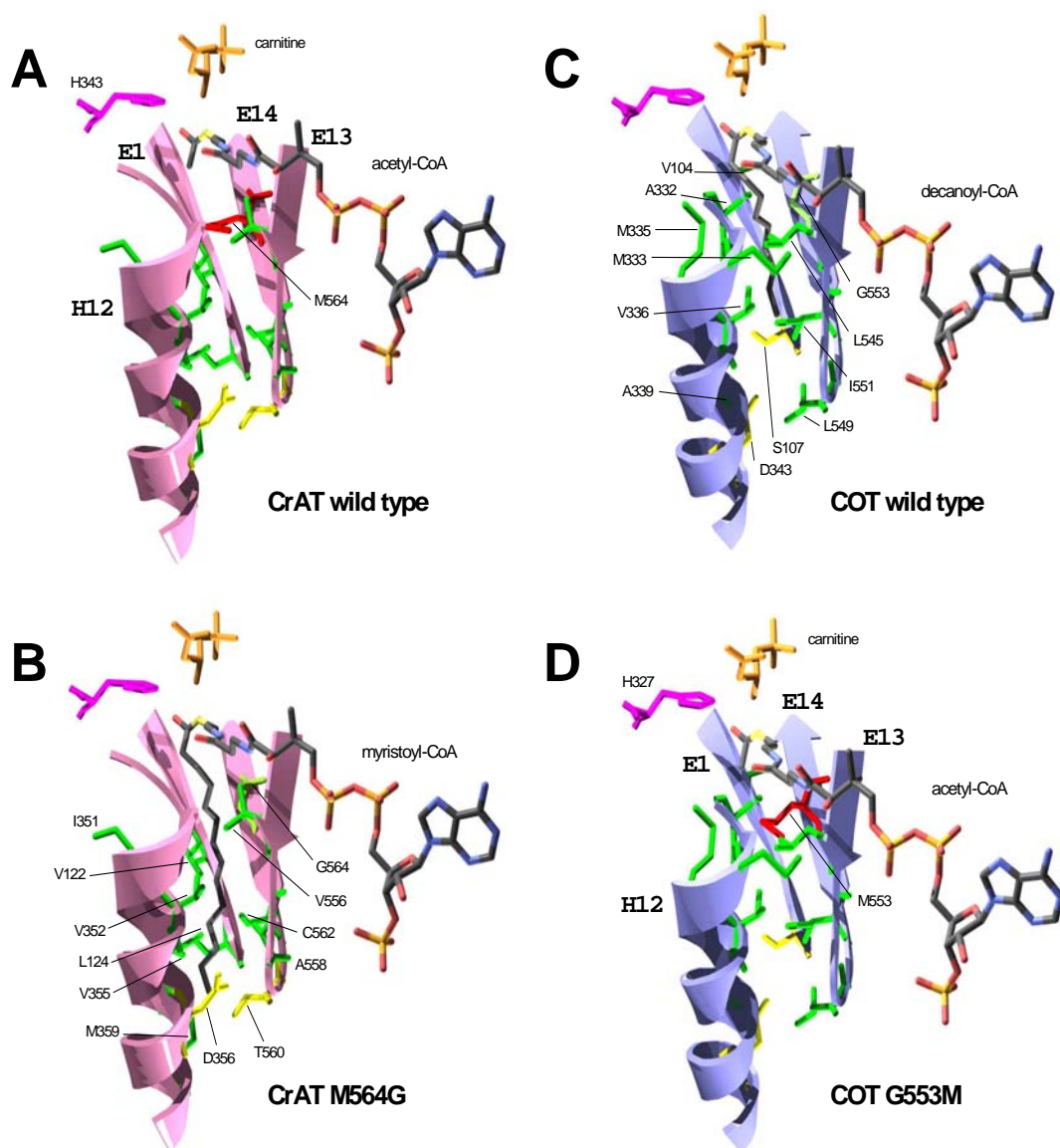


Fig. 19. Proposed models for the positioning of fatty acyl-CoAs in the wt and mutated CrAT and COT. (A) Location of a molecule of acetyl-CoA in the active center of wt CrAT. Position of Met⁵⁶⁴ (red) as well as the secondary structure elements α -helix H12 and β -strands E1, E13 and E14, surrounding the acetyl hollow, are indicated. The molecule of carnitine, as well as the catalytic residue His³⁴³ are also represented. (B) Location of a molecule of myristoyl-CoA in the deep pocket opened in the CrAT mutant M564G. Positions of Gly⁵⁶⁴, hydrophobic residues around the acyl-chain (Val¹²², Leu¹²⁴, Ile³⁵¹, Val³⁵², Val³⁵⁵, Met³⁵⁹, Val⁵⁵⁶, Ala⁵⁵⁸ and Cys⁵⁶²) and polar residues Asp³⁵⁶ and Thr⁵⁶⁰ are indicated. (C) A molecule of decanoyl-CoA in the hydrophobic pocket defined by α -helix H12 and β -strands E1, E13 and E14 of wt COT. Positions of Val¹⁰⁴, Ala³³², Met³³³, Met³³⁵, Val³³⁶, Ala³³⁹, Leu⁵⁴⁵, Leu⁵⁴⁹ and Ile⁵⁵¹ and the polar residues Ser¹⁰⁷ and Asp³⁴³ are indicated. (D) Model for the location of a molecule of acetyl-CoA in the shallow cavity closed by Met⁵⁵³ (red) of COT mutant G553M. Carnitine, His³²⁷ and the positions of secondary structure elements are also represented.

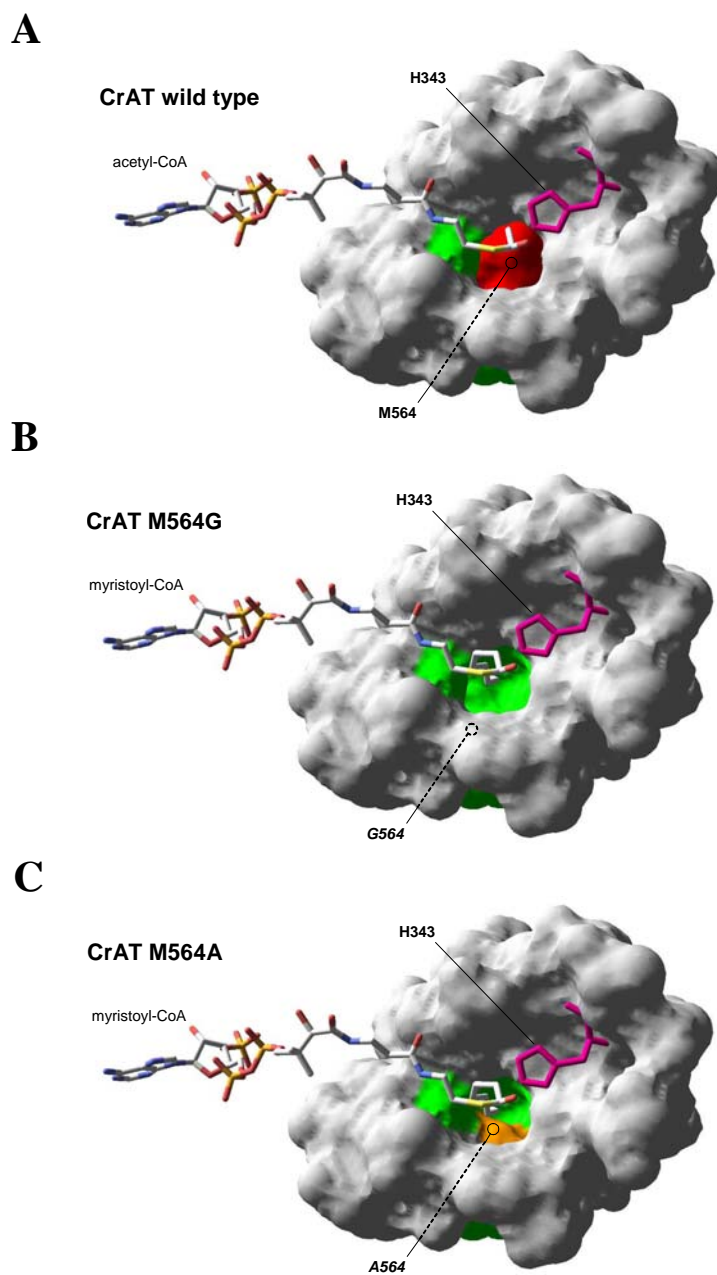


Fig. 20. **Substrate docking in wild-type CrAT and mutants.** Proposed location of acetyl-CoA and myristoyl-CoA acyl-chains in the active centres of rat CrAT wt (A), mutant M564G (B) and mutant M564A (C) surface structural models respectively. Hydrophobic residues in the walls of the deep pocket are coloured in green. Met⁵⁶⁴ surface, closing the cavity in wild-type CrAT, is depicted in red. Ala⁵⁶⁴ is depicted in yellow. Catalytic His³⁴³ is also represented (pink trace).

7.3. IDENTIFICATION OF A NEW AMINO ACID INVOLVED IN ACYL-CoA SPECIFICITY IN CrAT FROM THE MODELS

After a thorough examination of the 3-D model for the positioning of myristoyl-CoA in the CrAT M564G mutant (Fig. 19B), we identified one charged residue, Asp³⁵⁶, which conforms the putative bottom closure of the hydrophobic pocket and could hinder the correct positioning of acyl-CoAs longer than myristoyl-CoA. The presence of a polar residue at this position would explain why CrAT mutant M564G was very active with myristoyl-CoA but much less so with palmitoyl-CoA.

To create a more suitable environment for the acyl group of long-chain acyl-CoAs inside the hydrophobic pocket of CrAT, we decided to mutate Asp³⁵⁶ to the small, uncharged, hydrophobic alanine. The mutation was introduced by PCR using the primers CrAT D356A.for and CrAT D356A.rev and the pYESCrAT^{M564G} plasmid as template, resulting in the pYESCrAT^{D356A/M564G} construct. CrAT double mutant D356A/M564G was expressed in a *S. cerevisiae* strain devoid of endogenous CrAT, COT and CPT activity.

7.3.1. The D356A/M564G mutation converts CrAT into CPT

Enzyme activity of the yeast-expressed CrAT mutant D356A/M564G was tested for acyl-CoA substrates of various lengths from acetyl- to arachidoyl-CoA (C₂₀-CoA) and compared with CrAT mutant M564G (Table 9). CrAT mutant M564G was very active towards medium-chain acyl-CoAs, but its activity decreased dramatically towards palmitoyl-CoA, and was undetectable with stearoyl-CoA (C₁₈-CoA) and arachidoyl-CoA. CrAT double mutant D356A/M564G also showed maximum activity towards hexanoyl-CoA (246 nmol·min⁻¹·mg protein⁻¹), but in contrast it showed a 6-fold increase in activity towards palmitoyl-CoA and a new activity towards stearoyl-CoA (100 and 38.9 nmol·min⁻¹·mg protein⁻¹, respectively), when compared with the single mutant M564G. If we express the results for palmitoyl-CoA as its relative activity with respect to hexanoyl-CoA, this figure was 41% for the CrAT double mutant, but only 2% for the single mutant (Fig. 21A). Western-blot of yeast-expressed wt CrAT and mutants D356A/M564G and M564G showed the same molecular masses and similar expression levels (Fig. 21B).

Results

Acyl-CoA	Activity (nmol·min ⁻¹ ·mg protein ⁻¹)		
	wt	M564G	D356A/M564G
C ₂ -CoA	409 ± 48	234 ± 30	50.7 ± 4.0
C ₄ -CoA	518 ± 19	641 ± 3.2	138 ± 26
C ₆ -CoA	138 ± 15	802 ± 66	246 ± 15
C ₈ -CoA	61 ± 1.1	488 ± 24	127 ± 29
C ₁₀ -CoA	21 ± 5.7	136 ± 7.3	67.0 ± 0.7
C ₁₂ -CoA	6.0 ± 2.6	350 ± 5.0	150 ± 24
C ₁₄ -CoA	0.33 ± 0.07	409 ± 29	218 ± 9.0
C ₁₆ -CoA	0	18.0 ± 3.6	100 ± 19
C ₁₈ -CoA	0	0	38.9 ± 1.4
C ₂₀ -CoA	0	0	0

Table 9. Enzyme activities of wt CrAT and M564G and D356A/M564G mutants expressed in *S. cerevisiae*. Mitochondrial protein (5 µg) from yeast expressing wt CrAT and M564G and D356A/M564G mutants were assayed with acyl-CoAs of different carbon-chain lengths, ranging from C₂-C₂₀. Results are shown as the mean ± S.D. of three independent experiments.

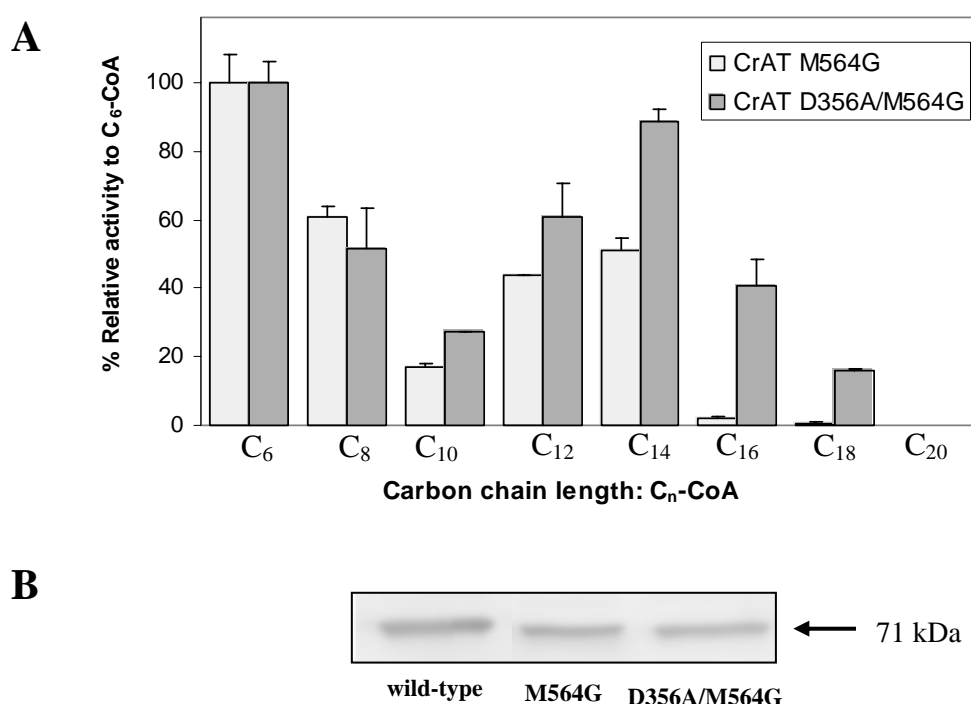


Fig. 21. Carnitine acyltransferase activity of yeast cells expressing CrAT mutant M564G and double mutant D356A/M564G. A) Mitochondrial protein (5 µg) from yeast expressing CrAT mutants M564G and D356A/M564G were assayed for activity with acyl-CoAs of different chain length ranging from C₆-C₂₀. The results are expressed as the relative acyl-CoA activity with regard to hexanoyl-CoA activity (scaled to 100). B) Immunoblots showing expression of wt CrAT, CrAT M564G and CrAT D356A/M564G. Yeast extracts (8 µg) were separated by SDS-PAGE and subjected to immunoblotting using specific antibodies. The arrow indicates the migration position and the molecular mass of rat CrAT.

In addition, yeast-expressed CrAT double mutant and L-CPT I wt activities were compared using a radiometric method (Materials and Methods, Section 7.2) with acyl-CoAs of different length from C₆- to C₂₀-CoA (Fig. 22). CrAT double mutant showed exactly the same activity as L-CPT I when C₁₂- and C₁₄-CoA were used as substrates. In longer acyl-CoAs, the CrAT double mutant displayed a similar activity toward palmitoyl-CoA, approximately 65% of that of L-CPT I wt (17.8 vs. 28 nmol·min⁻¹·mg protein⁻¹), whereas its activity with stearoyl-CoA was 25% of that of L-CPT I wt. The CrAT double mutant still maintained strong activity with C₆- and C₈-CoA as substrates, whereas L-CPT I activity toward acyl-CoAs with fewer than 10 carbons in their chain was much lower.

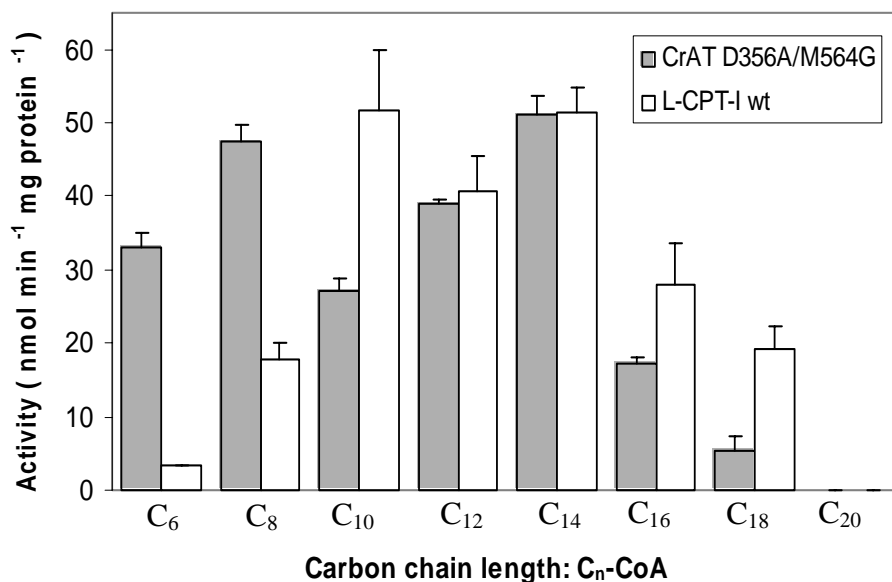


Fig. 22. Carnitine acyltransferase activity of *S. cerevisiae* cells expressing wild-type L-CPT I and CrAT double mutant D356A/M564G. Mitochondrial protein from yeast expressing L-CPT I and CrAT double mutant D356A/M564G were assayed for activity using a radiometric method with acyl-CoAs of different chain length ranging from C₆-C₂₀. Results are shown as the mean ± S.D. of three experiments.

These results indicate that the replacement of Asp³⁵⁶ with alanine (D356A), along with the mutation of Met⁵⁶⁴ to Gly, allows CrAT to catalyze long-chain acyl-CoAs such as palmitoyl- and stearoyl-CoA. The CrAT double mutant D356A/M564G catalyzes acyl-CoAs over a wide range of chain length, from acetyl- to stearoyl-CoA.

7.3.2. Kinetic characteristics of CrAT mutant D356A/M564G

We determined the kinetic parameters of CrAT mutant D356A/M564G with its novel substrate palmitoyl-CoA and its natural substrate acetyl-CoA (Table 10). The mutant showed standard saturation kinetics for both acyl-CoAs (Fig. 23).

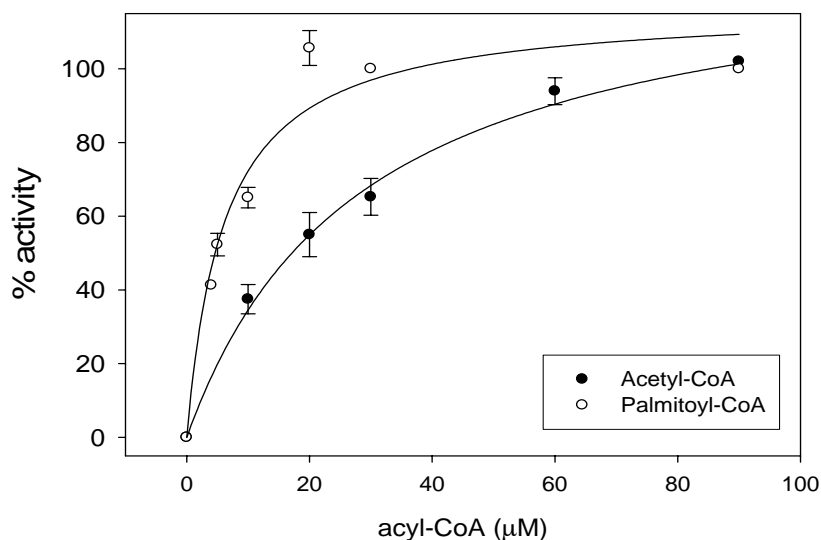


Fig. 23. **Acyl-CoA saturation curves for CrAT D356A/M564G expressed in yeast.** Mitochondrial protein (5 μg) from yeast-expressing CrAT D356A/M564G was assayed for activity at 1500 μM carnitine with increasing concentrations of acetyl- or palmitoyl-CoA. Results are shown as the mean ± S.D. of three experiments.

K_m values with acetyl- and palmitoyl-CoA were 23 μM and 7.2 μM, respectively, indicating a preference for long-chain acyl-CoAs. Furthermore, the K_m of this double mutant with palmitoyl-CoA was very similar to that of L-CPT I wt, 5.7 μM (Morillas, 2004). The catalytic efficiency when acetyl-CoA was the substrate was 2.9, whereas with palmitoyl-CoA it was 19.2, which again shows that the double CrAT mutant prefers long-chain acyl-CoAs.

Acyl-CoA	K_m (μM)	V_{max} (nmol·min ⁻¹ ·mg protein ⁻¹)	Catalytic efficiency (V_{max} / K_m)
C ₂ -CoA	23.0 ± 3.1	66.5 ± 2.1	2.9
C ₁₆ -CoA	7.2 ± 0.4	138 ± 25	19.2

Table 10. **Kinetic parameters of rat CrAT mutant D356A/M564G expressed in *S. cerevisiae*.** Mitochondrial protein (5 μg) from yeast expressing CrAT mutant D356A/M564G was assayed with acetyl- and palmitoyl-CoA. Results are shown as the mean ± S.D. of three independent experiments.

7.3.3. Positioning of long-chain acyl-CoAs in the CrAT mutant D356A/M564G

As described in Section 7.2, a 3-D model was proposed for the location of myristoyl-CoA in the hydrophobic pocket of CrAT mutant M564G (Fig. 19B). Refined *in silico* docking techniques were used in the present improved model, allowing free rotation of the acyl chain bonds of the ligands. This ensured a complete scan of the available conformational space inside the enzyme cavity. The new model for the position of myristoyl-CoA (Fig. 24A) is similar to the previous model, locating the acyl chain in the cavity that is open when Met⁵⁶⁴ is replaced by Gly. The bottom of the pocket is defined by the presence of Thr⁵⁶⁰, which closes the enzyme wall to the external surface, and Asp³⁵⁶, which prevents correct positioning of acyl-CoAs longer than myristoyl-CoA.

The bigger cavity formed in CrAT mutant D356A/M564G by replacing the larger, charged Asp³⁵⁶ with the tiny, non-polar alanine, allows the positioning of longer-chain acyl-CoAs. This has also been calculated, using the same *in silico* docking method, for palmitoyl-CoA (data not shown) and for stearoyl-CoA (Fig. 24B). The last four carbon atoms of the acyl chain of stearoyl-CoA form a U-turn, which avoids collision with Thr⁵⁶⁰ at the bottom of the tunnel and accommodates them in the space available around the substituted Ala³⁵⁶. When the docking of very-long chain acyl-CoAs, such as arachidoyl-CoA, into the large cavity of the CrAT D356A/M564G mutant was carried out, no models with low (stable) energy were obtained despite using the minimum constraints of appropriate location of the substrate to the enzyme active site. This indicates that the available space was too small to accommodate acyl chains of more than 18 atoms in length. The U-turn formed by stearoyl-CoA points towards the residues in the α -helix H12 (Fig. 24B), leaving no free space for additional carbon atoms of longer acyl chains. The absence of an appropriate model is consistent with the lack of activity of the D356A/M564G mutant enzyme towards arachidoyl-CoA (Fig. 21A). The positioning of the fatty acyl part of stearoyl-CoA is very similar to that modeled for the palmitoyl part of palmitoyl-CoA in the hydrophobic pocket of CPT I (Fig. 24C). Although the orthologous residue corresponding to CrAT Asp³⁵⁶ is also a charged residue in CPT I (Glu⁴⁸⁶), it does not interfere with the substrate position due to the wider cavity conformed by the naturally adopted structural elements, including the distinctive long and flexible loop between β -strands E13 and E14.

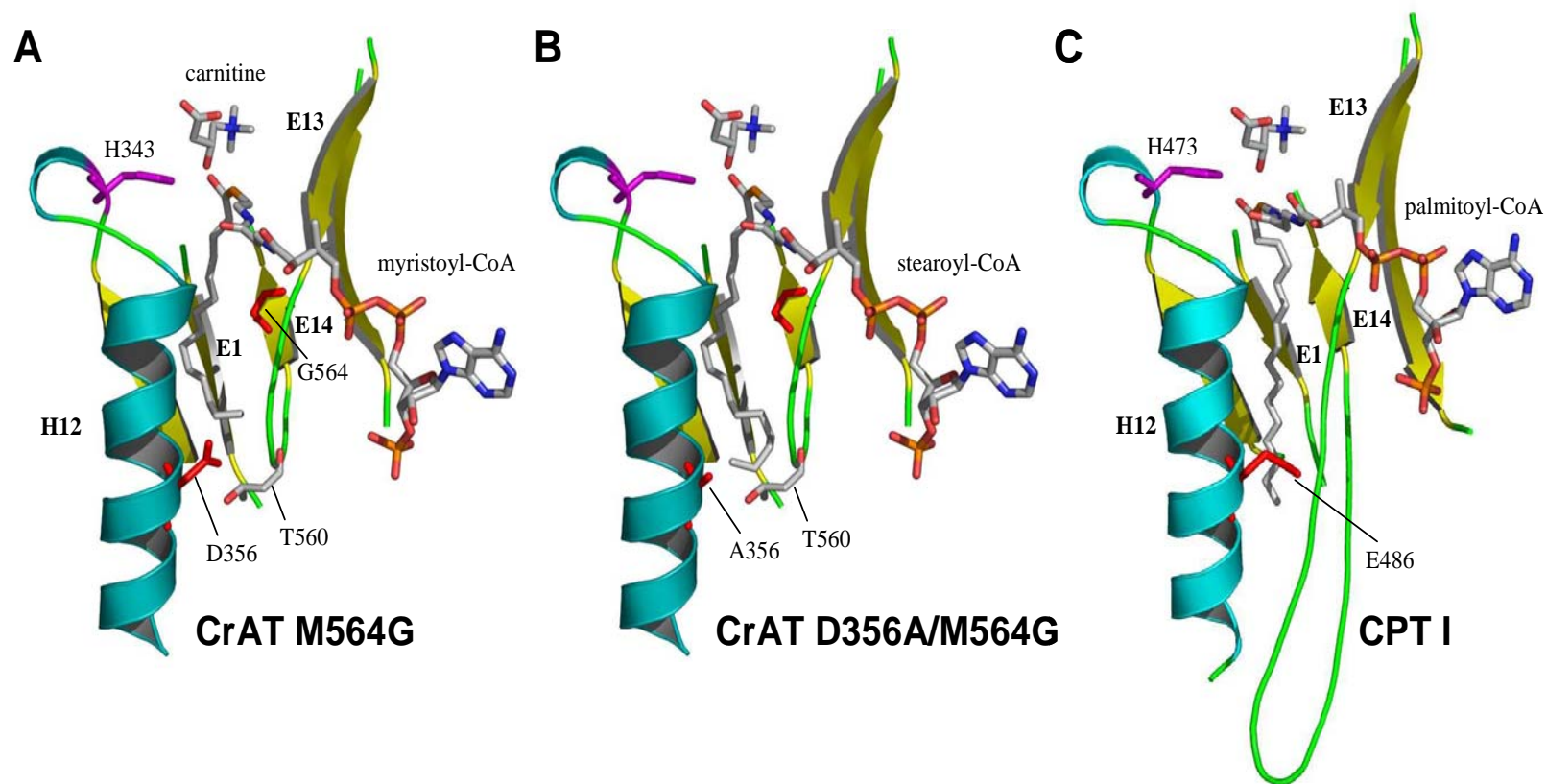


Fig. 24. **Proposed models for the positioning of long-chain acyl-CoAs in CrAT mutants M564G and D356A/M564G and wt L-CPT I.** A) Location of a myristoyl-CoA molecule in the pocket opened in the CrAT mutant M564G. B) Location of a stearoyl-CoA molecule in the deep pocket opened in the CrAT mutant D356A/M564G. Position of residues Gly⁵⁶⁴ and Asp³⁵⁶ or Ala³⁵⁶ (red) as well as Thr⁵⁶⁰, the catalytic His³⁴³ (magenta) and the molecule of carnitine are indicated. Secondary structure elements are also represented (alpha helix H12 in blue, beta strands in yellow). C) Model for the location of a molecule of palmitoyl-CoA in CPT I.

8. EFFECT OF CPT I INHIBITORS MALONYL-CoA AND C75-CoA ON THE ACTIVITY OF CrAT EXPRESSED IN YEAST

8.1. EFFECT OF MALONYL-CoA ON CrAT ACTIVITY

It is well-known that malonyl-CoA is a physiological inhibitor of CPT I and COT proteins, but in contrast, it has no effect on CrAT activity. As we had converted rat CrAT into a pseudo-COT (mutant M564G) and a pseudo-CPT (mutant D356A/M564G) in terms of acyl-CoA selectivity, we wanted to determine whether any of these mutants had also acquired a new sensitivity towards malonyl-CoA. With this purpose, we carried out experiments for competitive inhibition with wt CrAT and mutants.

Increasing concentrations of malonyl-CoA were incubated with yeast-expressed wt CrAT and mutants. Malonyl-CoA had almost no effect on wt CrAT activity with acetyl-CoA as the substrate, and the same was observed in the M564G and D356A/M564G mutants with myristoyl-CoA (Fig. 25). At a concentration of 100 μ M malonyl-CoA, the remaining CrAT activity was 84% for wt CrAT, 83% for M564G, and 72% for D356A/M564G. At the same concentration, L-CPT I activity is almost completely abolished (Morillas, 2003).

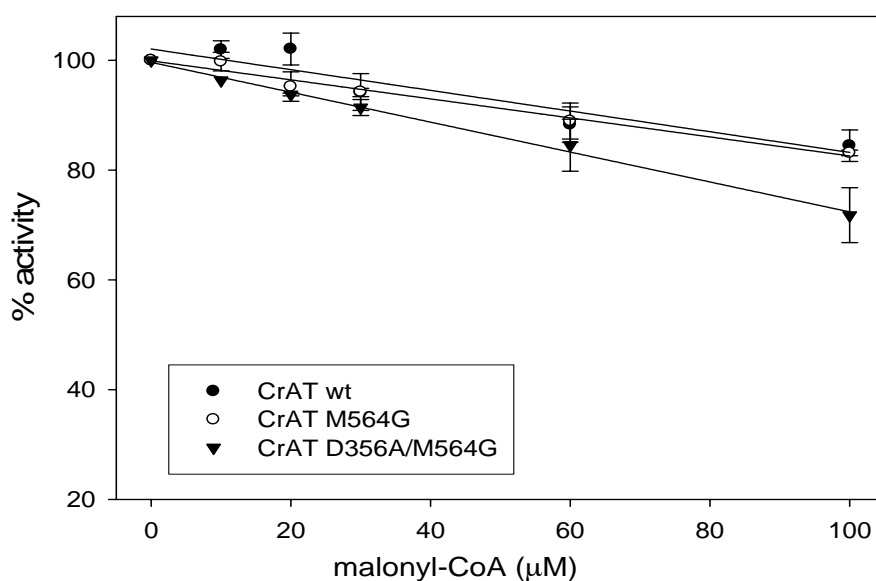


Fig. 25. **Effects of malonyl-CoA on the activity of wt and mutated CrAT.** Mitochondrial protein from yeast expressing wt CrAT and CrAT mutants M564G and D356A/M564G were preincubated for 5 min with increasing concentrations of malonyl-CoA. CrAT activity was measured and data are expressed relative to control values in absence of the drug (100%) as the mean of three independent experiments.

8.2. EFFECT OF C75-CoA ON CrAT ACTIVITY

C75 has been described as a malonyl-CoA analogue that antagonizes the allosteric inhibitory effect of malonyl-CoA on CPT I (Thupari, 2002). In our group, it has been demonstrated that, unlike the activation produced by C75, its CoA derivative is a potent and competitive inhibitor of CPT I (Bentebibel, 2006). *In silico* molecular docking studies showed that C75-CoA occupies the same pocket in CPT I as palmitoyl-CoA, suggesting an inhibitory mechanism based on mutual exclusion.

Taking into account the previous considerations, we hypothesised that in the same way that C75-CoA occupies the fatty acid binding site of CPT I, it would also fit in the open hydrophobic pocket formed in CrAT mutants M564G and D356A/M564G, but not in the shallow cavity of wt CrAT. Thus, C75-CoA might compete with acyl-CoA substrates to bind in the fatty acid binding site of CrAT mutants M564G and D356A/M564G, and might act as a competitive inhibitor.

To assess the relationship between C75-CoA and the substrate acyl-CoA, we carried out experiments for competitive inhibition with wt CrAT and mutants using a radiometric assay. Acetyl-CoA and myristoyl-CoA were used as substrates for wt CrAT and CrAT mutants, respectively. To activate C75 into C75-CoA, the drug was incubated in the presence of CoA and acyl-CoA synthetase, as described in Material and Methods (Section 7.2.2.1). Excess CoA from the C75-CoA activation solution was removed since it has been shown that CrAT activity is inhibited by its product CoA (Huckle, 1983).

Increasing concentrations of synthesized C75-CoA were incubated with yeast-overexpressed mitochondrial wt CrAT and mutants M564G and D356A/M564G. C75-CoA inhibited CrAT mutants M564G and D356A/M564G but almost had no effect on wt CrAT (Fig. 26). At a concentration of 60 μ M C75-CoA, the remaining CrAT activity was 83% for wt CrAT, 45% for CrAT mutant M564G, and as low as 21% of the original level for CrAT mutant D356A/M564G.

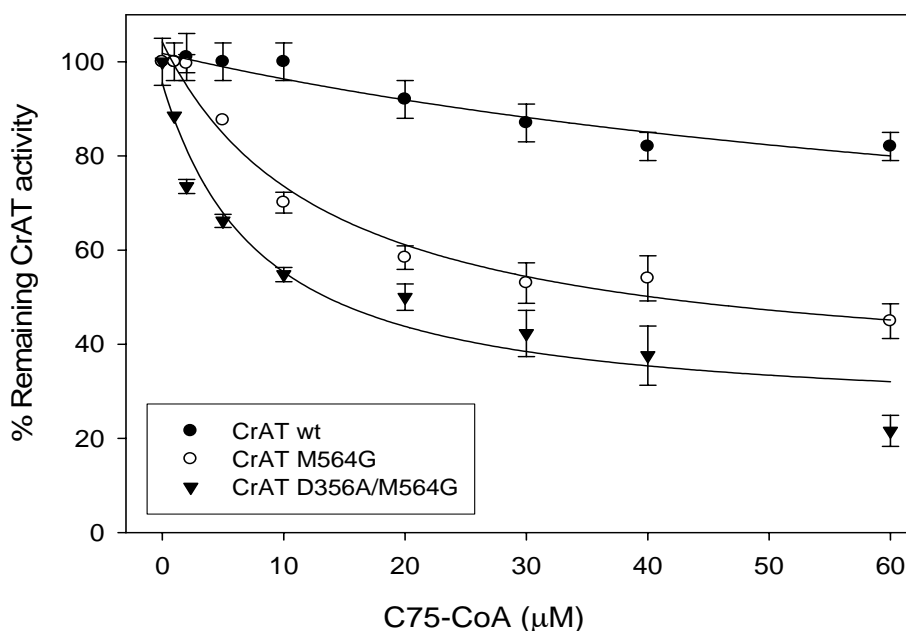


Fig. 26. **Effects of C75-CoA on the activity of wt and mutated CrAT.** Mitochondrial protein from yeast expressing wt CrAT and CrAT mutants M564G and D356A/M564G were preincubated for 5 min with increasing concentrations of C75-CoA. CrAT activity was measured and data are expressed relative to control values in the absence of the drug (100%) as the mean of three independent experiments.

Drug concentrations ranging from 1 to 60 μM were used to estimate the IC_{50} value. IC_{50} corresponds to the concentration of inhibitor that inhibits 50% of the enzyme activity. IC_{50} values for C75-CoA were 44.4 μM for CrAT mutant M564G and 12.8 μM for the D356A/M564G mutant (Table 11). C75-CoA appears to be a stronger inhibitor of the CrAT double mutant D356A/M564G than the M564G mutant, although both CrAT mutants are less sensitive to C75-CoA than L-CPT I ($\text{IC}_{50} = 0.24 \mu\text{M}$) (Bentebibel, 2006).

The inhibitor-binding affinity (K_i) was also estimated by nonlinear regression analysis, as described in Materials and Methods (Section 7.2.2.2). Because inhibitory potency is linearly related to the binding affinity, the K_i is a valuable predictor of in vivo potency. The K_i values were estimated to be 22.9 and 4.39 μM for CrAT mutants M564G and D356A/M564G, respectively (Table 11). These figures show that the CrAT double mutant binds C75-CoA more tightly than the single mutant. The K_i value for C75-CoA acting on L-CPT I (0.23 μM) was 19-fold lower than that observed for CrAT mutant D356A/M564G (Bentebibel, 2006). It was not possible to calculate the IC_{50} and K_i values for wt CrAT due to the lack of inhibition by C75-CoA.

Results

Enzyme	Acyl-CoA assayed	C75-CoA inhibition	
		IC ₅₀ (μM)	K _i (μM)
CrAT wt	C ₂ -CoA	∞	∞
CrAT M564G	C ₁₄ -CoA	44.4 ± 11.3	22.9 ± 6.0
CrAT D356A/M564G	C ₁₄ -CoA	12.8 ± 2.2	4.39 ± 0.67

Table 11. **IC₅₀ and K_i values of wt and mutated CrAT for C75-CoA.** Mitochondrial fractions obtained from yeast overexpressing wt CrAT and CrAT mutants M564G and D356A/M564G were assayed for activity in the presence of C75-CoA. IC₅₀ and K_i values were calculated as described in Materials and methods. ∞: infinite.

9. NEW MODEL FOR THE POSITIONING OF FATTY ACIDS IN RAT COT BASED ON THE CRYSTAL STRUCTURE OF MOUSE COT

Previously, we had proposed a model for rat COT based on the 3-D structure of CrAT (Sections 7.1 and 7.2). After publication of the crystal structure of mouse COT (Jogl, 2005), a new structural model of the rat COT was generated by homology-modeling procedures using the crystal structure of mouse COT as a template (PDB entry 1XL7), as described in Materials and Methods (Section 8.4). The root mean square distance between equivalent C_{α} atoms of mouse COT and modelled rat COT structures is 0.07\AA , which confirms that the models for each of the enzymes are virtually identical in terms of backbone similarity. The octanoylcarnitine molecule was located in the model using the information available in the crystallized structures of mouse COT in complex with octanoylcarnitine (PDB entry 1XL8). A structural alignment of the new model with the former one based on the crystal structure of CrAT revealed minor differences (Fig. 27A).

9.1. THE BINDING SITE FOR MEDIUM-CHAIN ACYL GROUPS IN RAT COT

The location of octanoylcarnitine in the active site of the model for rat wt COT (Fig. 27B) is very similar to that described in the crystallized mouse COT. The binding pocket is lined along its entire length with hydrophobic residues. These residues define a cylindrical-shaped binding site, which represents a good fit to the contour of the acyl groups. As observed in mouse CrAT, the side chain of Met³³⁵ interacts with the C8 atom of the octanoyl group and could possibly interfere with the correct positioning of the acyl group of long-chain acyl-CoAs inside the hydrophobic pocket of COT (Jogl, 2005).

Based on the position of octanoylcarnitine in the model, a putative orientation for acyl-groups longer than eight carbons can be proposed within the hydrophobic pocket (indicated with a dashed yellow line in the model). The extended acyl-chain would then clash with the side chains of a series of amino acids that are oriented toward the longitudinal axis of the hydrophobic channel. Thus, the side chains of Ile⁵⁵¹ and Asp³⁴³ would probably interfere with the correct positioning of acyl-groups longer than eight

carbons and might determine the substrate selectivity of COT toward medium-chain acyl-CoAs. The Asp³⁴³ in COT is situated just a few Å below the structurally homologous Asp³⁵⁶ in CrAT, a residue which plays an important role in determining the acyl-CoA preference of CrAT (section 7.3.1). Moreover, this Asp³⁴³ defines the bottom closure of the hydrophobic pocket in the rat COT model, along with Leu³⁴⁶ and His¹⁰⁹.

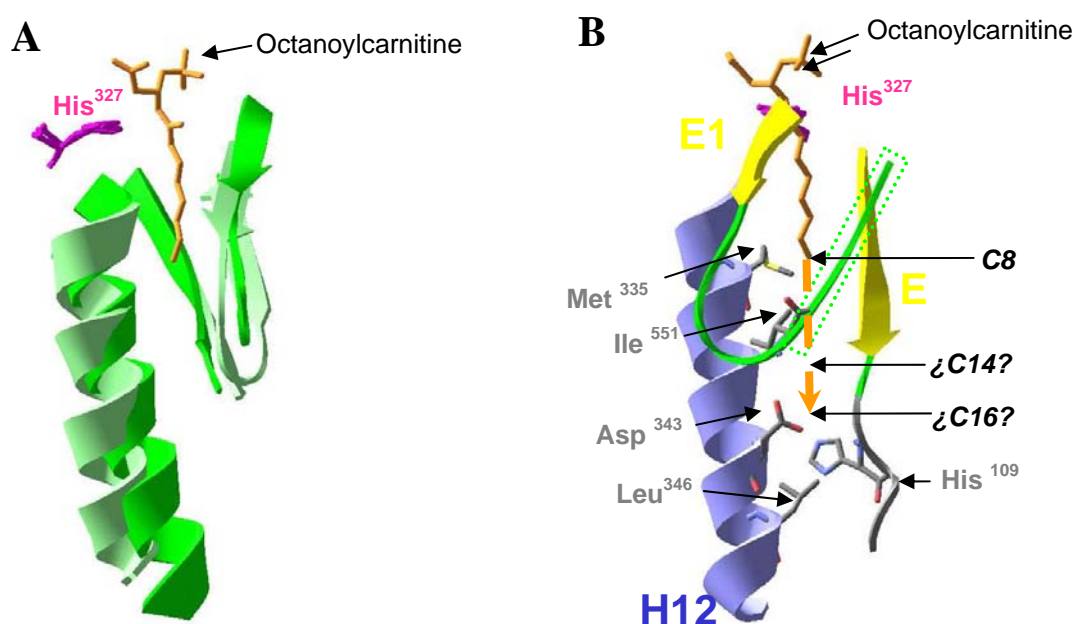


Fig. 27. Proposed model for the positioning of medium- and long-chain acyl-CoAs in rat wt COT. A) Structural alignment of the models for rat COT based on CrAT and COT crystals (depicted in pale and bright green, respectively). B) Location of a molecule of octanoylcarnitine in the hydrophobic pocket defined by α -helix H12 and β -strands E1, E13 and E14 of wt COT. Putative orientation for acyl-groups longer than eight carbons within the hydrophobic pocket is indicated with a dashed orange line. Position of the conserved residues in COT subfamily possibly interfering with accommodation of long aliphatic groups within the hydrophobic pocket are indicated (His¹⁰⁹, Met³³⁵, Asp³⁴³, Leu³⁴⁶, and Ile⁵⁵¹). The catalytic histidine, His³²⁷, and the positions of secondary structure elements are also shown.

To assess the functional relevance of Ile⁵⁵¹ and Asp³⁴³, we decided to create single-site mutants of rat COT (COT mutants I551A and D343A). Both amino acids were individually replaced with the small and uncharged Ala to create a more suitable environment for the positioning of long-chain acyl-CoAs. The mutations were introduced using a PCR-based mutagenesis procedure with the pYESCOT^{wt} plasmid as template. The primers COT I551A.for and COT I551A.rev were used to construct pYESCOT^{I551A}, and primers COT D343A.for and COT D343A.rev were used to construct pYESCOT^{D343A}. Both plasmids were expressed in an *S. cerevisiae* strain devoid of carnitine acyltransferase activity. Western-blot of yeast-expressed wt COT

and mutants D343A and I551A showed the same molecular mass and similar expression levels (Fig. 28B).

Enzyme activity of yeast-expressed COT mutants I551A and D343A were tested for acyl-CoA substrates of various lengths from hexanoyl- to palmitoyl-CoA and compared with wt COT (Fig 28A). The kinetic data showed that COT mutant D343A had slightly lower catalytic activity but maintained the same substrate preference as the wild-type enzyme. Somewhat unexpectedly, our kinetic experiments showed that the I551A mutant had significantly reduced catalytic activity with all the acyl-CoAs substrates assayed and its activity with long-chain acyl-CoAs was very low. Thus, the kinetic data suggest that neither mutant displays enhanced activity with the long-chain substrates.

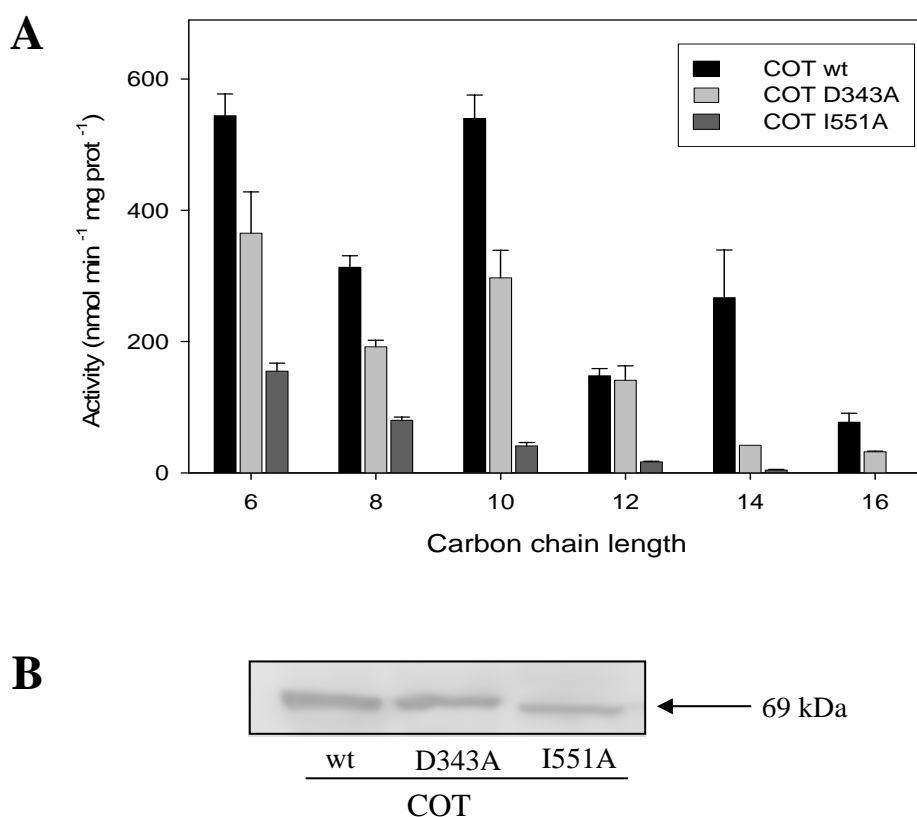


Fig. 28. **Carnitine acyltransferase activity of *S. cerevisiae* cells expressing wild-type COT and mutants D343A and I551A.** Protein extracts from yeast expressing wt COT and COT mutants D343A and I551A were assayed for activity with acyl-CoAs of different carbon-chain lengths, ranging from C₆-C₁₆. Results are shown as the mean \pm S.D. of three independent experiments. B) Immunoblots showing expression of wt COT, COT D343A and COT I551A. Yeast protein extracts (10 μ g) were separated by SDS-PAGE and subjected to immunoblotting using specific antibodies. The arrow indicates the migration position and the molecular mass of rat COT.

10. CARNITINE/CHOLINE DISCRIMINATION IN CrAT

Taking into consideration the structural information revealed by the recent publication of the crystal structure of rat ChAT (Cai, 2004; Govindasamy, 2004) and mutagenesis studies (Cronin 1997a; Cronin, 1998), we attempted to redesign CrAT to use choline as the acceptor of the acetyl group instead of its natural substrate carnitine. First, we prepared the CrAT triple mutant T465V/T467N/R518N (TM), which incorporates the reverse substitutions that Cronin (1998) successfully performed in rat ChAT and allowed ChAT to accommodate carnitine instead of choline. The triple mutant was expected to eliminate most of the interactions between CrAT and the carboxylate group of carnitine since Thr⁴⁶⁵ and Arg⁵¹⁸ interact with this negatively charged group, which might favor the binding of choline.

At the same time, however, this triple mutant might increase the volume of the catalytic site of CrAT, which could interfere with the correct positioning of the smaller choline. Therefore, to reduce the volume of the carnitine binding pocket and create a more favorable environment to accommodate the choline, we prepared the CrAT quadruple mutant A106M/T465V/T467N/R518N (QM), with the additional replacement of Ala¹⁰⁶ with Met (Ala¹⁰⁶ in CrAT substitutes for the bulkier Met⁹⁴ in ChAT). The mutations were introduced using a PCR-based mutagenesis procedure with the pGEX-CrAT^{wt} plasmid as template. Wild-type CrAT, CrAT TM and CrAT QM were expressed in a soluble form in *E. coli* and the protein was purified to homogeneity, as described in Materials in Methods (Section 3).

10.1. RE-ENGINEERING CrAT INTO ChAT

Enzyme activity of the *E. coli*-expressed wild-type CrAT and CrAT triple and quadruple mutants was analysed with the substrate pairs choline/acetyl-CoA and carnitine/acetyl-CoA (Table 12). The mutations led to an impairment in activity toward carnitine: a maximal 400-fold reduction in the QM compared with wild-type and a 146-fold reduction in the TM. In contrast to the results obtained with carnitine, both CrAT mutants showed improved activity towards choline (3-fold) when compared with the wild-type enzyme.

Results

CrAT	Activity	
	L-carnitine	Choline
nmol min ⁻¹ mg protein ⁻¹		
wt	43,270 ± 5,400	328 ± 51
TM	294 ± 7.9 (↓ 146)	876 ± 53 (↑ 3)
QM	108 ± 5.6 (↓ 400)	920 ± 70 (↑ 3)

Table 12. Enzyme activity of wild-type CrAT, CrAT triple mutant T465V/T467N/R518N (TM) and quadruple mutant A106M/T465V/T467N/R518N (QM) expressed in *E. coli*. Results are shown as the mean ± S.D. of three independent experiments. L-carnitine and choline were used in the assay at a concentration of 20 mM. The values in parentheses represent the fold change of the activity compared with that of wild-type.

Kinetic experiments were also performed with the substrate pairs choline/acetyl-CoA and carnitine/acetyl-CoA (Table 13). The wt enzyme and both mutants showed standard saturation kinetics for all the substrates tested, with the exception of the triple and quadruple mutants with carnitine (Fig. 29).

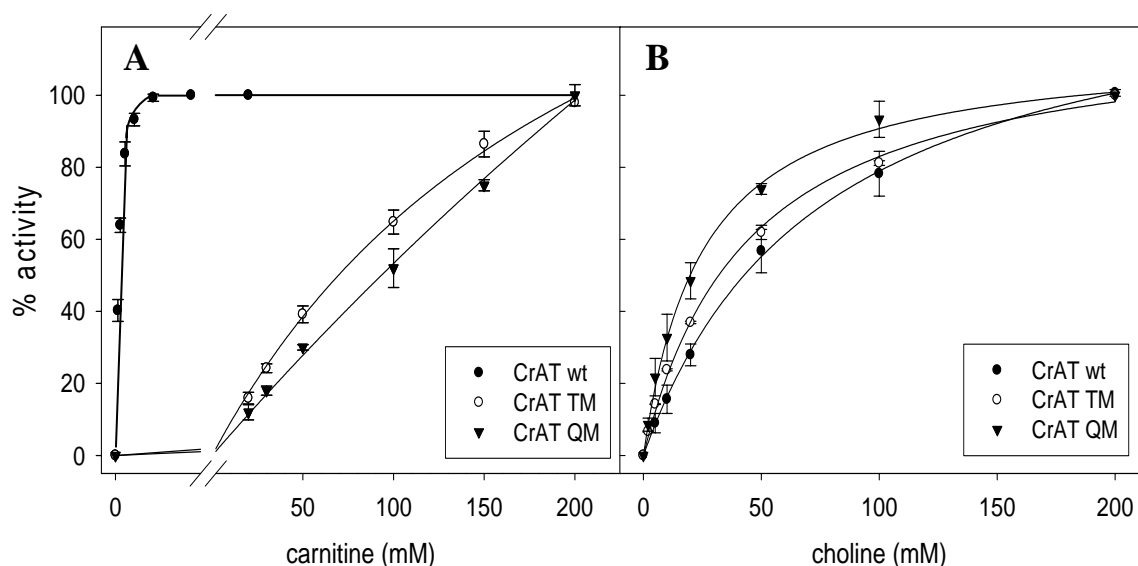


Fig. 29. Carnitine and choline saturation curves for wild-type CrAT and CrAT triple mutant T465V/T467N/R518N (TM) and quadruple mutant A106M/T465V/T467N/R518N (QM) expressed in *E. coli*. Purified protein from *E. coli* expressing wt CrAT and triple and quadruple mutants was assayed for activity at 100 μ M acetyl-CoA with increasing concentrations of carnitine (A) or choline (B). Results are shown as the mean ± S.D. of three independent experiments.

Both CrAT mutants showed improved catalytic efficiency towards choline (defined as K_{cat}/K_m) when compared with wt, and this increase was higher in the QM (9-fold) than in the TM (5-fold). In both mutants, the increase in catalytic efficiency was more influenced by the lowering of the K_m value towards choline (5-fold in the QM and 3-fold in the TM) than by an increase in K_{cat} (Table 13).

In contrast to the results with choline, the two mutants reduced the catalytic efficiency towards carnitine. Again, the greatest effect occurred with the quadruple mutant, with a decrease of more than five orders of magnitude (640,000-fold) in catalytic efficiency compared with wt, whereas the reduction in the triple mutant was about 75,000-fold. This impairment in catalytic efficiency towards carnitine is due to the combination of a decrease in K_{cat} and an increase in K_m towards carnitine, the latter being the stronger factor.

Comparison of the catalytic efficiencies between choline and carnitine for each enzyme derivative shows that while CrAT wt prefers carnitine over choline as the acceptor of the acetyl moiety by a factor of 47,000 (8.6×10^5 vs. $18.2 \text{ M}^{-1}\text{s}^{-1}$), the mutation of four amino acid residues in CrAT shifts the catalytic discrimination of the enzyme in favor of choline. Thus, the QM acetylates choline with a higher catalytic efficiency than carnitine by a factor of 128 (172 vs. $1.34 \text{ M}^{-1}\text{s}^{-1}$).

In the CrAT triple and quadruple mutants, K_m values for acetyl-CoA in the presence of carnitine and choline were very similar to those of wt CrAT (Table 13). When carnitine was used, K_m values for acetyl-CoA were $39 \mu\text{M}$ for the wt CrAT, $33 \mu\text{M}$ for the TM and $28 \mu\text{M}$ for the QM. In the presence of choline, K_m values for acetyl-CoA were $19 \mu\text{M}$ for wt CrAT, $26 \mu\text{M}$ for the TM and $28 \mu\text{M}$ for the QM. These results indicate that none of the mutations had any effect on the affinity of the enzyme for acetyl-CoA.

Results

CrAT	Substrate pair	K_m	K_{cat}	Catalytic efficiency (K_{cat}/K_m)
		μM	s^{-1}	$\text{M}^{-1} \cdot \text{s}^{-1}$
<i>wt</i>	Acetyl-CoA	39.1 ± 2.6	86.9 ± 3.6	2.22×10^6
	Carnitine	101 ± 4.6		8.60×10^5
	Acetyl-CoA	18.4 ± 1.3	1.58 ± 0.14	8.56×10^4
	Choline	$86,400 \pm 5,300$		1.82×10^1
TM	Acetyl-CoA	32.7 ± 3.6^a	2.97 ± 0.07	9.09×10^4 (↓ 24)
	Carnitine	$260,000 \pm 19,000$		1.14×10^1 (↓ 75,000)
	Acetyl-CoA	25.9 ± 0.6	2.43 ± 0.10	9.36×10^4 (1)
	Choline	$29,000 \pm 4,200$		8.37×10^1 (↑ 5)
QM	Acetyl-CoA	28.3 ± 3.2^a	0.98 ± 0.08	3.44×10^4 (↓ 264)
	Carnitine	$> 300,000$		1.34 (↓ 640,000)
	Acetyl-CoA	31.8 ± 5.2	3.11 ± 0.19	9.76×10^4 (1)
	Choline	$18,100 \pm 330$		1.72×10^2 (↑ 9)

Table 13. **Kinetic parameters of rat CrAT in *E. coli* cells expressing wild-type CrAT, CrAT triple mutant T465V/T467N/R518N (TM) and quadruple mutant A106M/T465V/T467N/R518N (QM).** Purified protein from *E. coli* expressing wt CrAT and triple and quadruple mutants were assayed for kinetics. Results are shown as the mean \pm S.D. of three independent experiments. The values in parentheses represent the fold change of the catalytic efficiency (K_{cat}/K_m) versus that of wild-type. ^aApparent value determined at a subsaturating concentration (100 mM) of carnitine.

10.2. MODELS OF CARNITINE AND CHOLINE BINDING SITES

In an attempt to understand the characteristics of the carnitine/choline binding site in CrAT, 3-D models were built for the wt and the triple and quadruple CrAT mutants and compared with the published structures of rat ChAT (Govindasamy, 2004; Cai, 2004). Using rigid docking techniques, location of both substrates was calculated for the active site of each enzyme (Fig. 30). According to the models, the electrostatic characteristics of the substrate site for the triple mutant CrAT resemble wt ChAT more than wt CrAT. In addition to the lack of specific contact for the carboxylate group of carnitine, the site for the trimethylammonium group, common to both substrates, is maintained. In the quadruple mutant, the presence of Met instead of the original Ala¹⁰⁶ mimics the wt ChAT active site almost completely. The reduction of the size of the tunnel impedes the entry of carnitine and allows better positioning of the smaller choline.

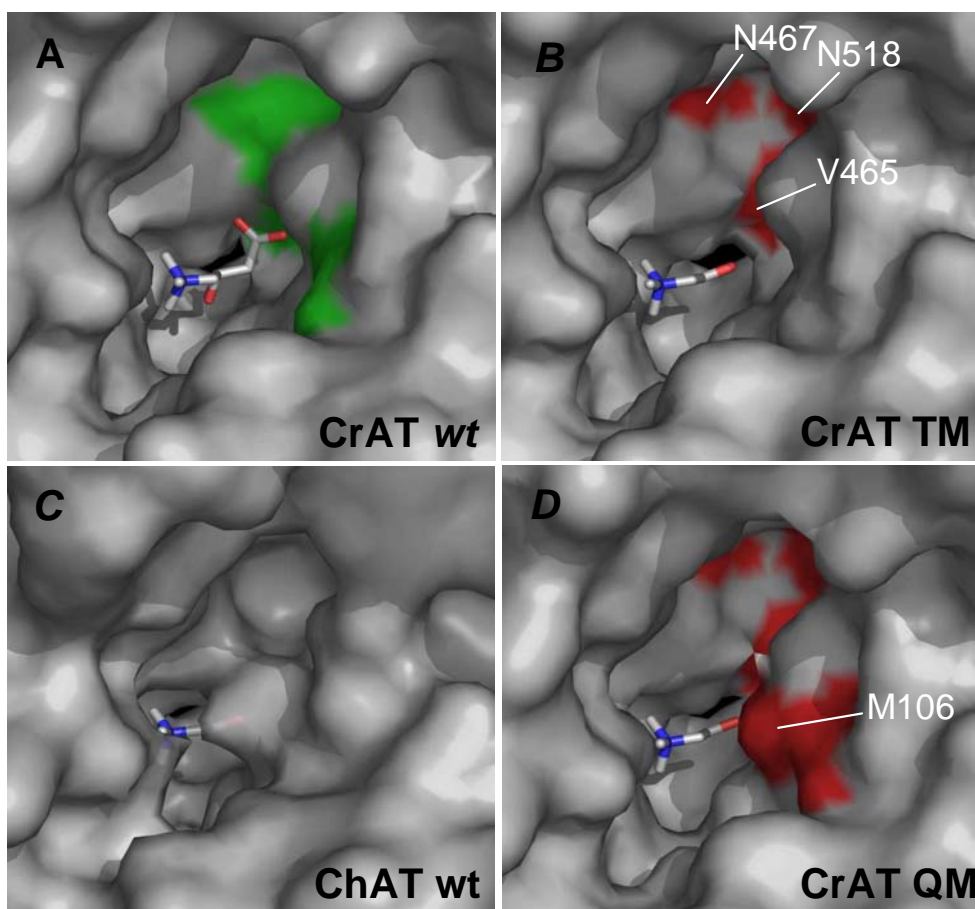


Fig. 30. **Models of substrate binding sites for wt CrAT, CrAT TM and CrAT QM compared to the active site of rat wt ChAT.** Representation of the protein surface of the entrance tunnel for carnitine/choline substrates for wt CrAT (A), CrAT triple mutant (TM) (B), CrAT quadruple mutant (QM) (D) and wt ChAT structure (C). The location of a molecule of carnitine is shown in the wt CrAT model, whereas a molecule of choline is shown in CrAT TM, CrAT QM, and wt ChAT. Vacuum electrostatics for active sites was calculated and represented using PyMOL (DeLano, 2002). Approximate positions of mutated residues Met¹⁰⁶, Val⁴⁶⁵, Asn⁴⁶⁷, and Asn⁵¹⁸ are indicated in red. The approximate positions of Ala¹⁰⁶, Thr⁴⁶⁵, Thr⁴⁶⁷, and Arg⁵¹⁸ in wt CrAT are shown in green.

11. BIOTECHNOLOGICAL APPLICATIONS OF CARNITINE ACETYLTRANSFERASE

11.1. CARNITINE ACETYLTRANSFERASE ACTIVITY AND ESTER PRODUCTION IN YEAST

Volatile aroma-active esters are largely responsible for the fruity character of wine. Esters are produced by fermenting yeast cells in an enzyme-catalyzed reaction between a higher alcohol and an acyl-CoA molecule (Swiegers, 2005). It has been shown that the rate of ester production rate is influenced, among other factors, by the concentration of the two co-substrates: an alcohol and acetyl-CoA (Verstrepen, 2003a; Horton, 2003). Since carnitine acetyltransferase is responsible for the modulation of the acyl-CoA/CoA ratio, we hypothesized that an overexpression of this enzyme in yeast could modify acyl-CoA levels and, therefore, ester levels.

S. cerevisiae contains three genes coding for carnitine acetyltransferase activity: *CAT2*, *YAT1* and *YAT2* (Kispal, 1993; Schmalix, 1993; Swiegers, 2001). We decided to overexpress *CAT2* since it is the most well-known CrAT gene, and the protein encoded by this gene, Cat2p, accounts for more than 95% of total CrAT activity in yeast cells grown on oleate or galactose (Elgersma, 1995; Kispal, 1993).

11.2. ISOLATION AND CLONING OF THE YEAST *CAT2* GENE

Genomic DNA was isolated from a widely used commercial wine yeast strain of *S. cerevisiae*, VIN13, as described in Materials and Methods (Section 2.9). Yeast *CAT2* was amplified from VIN13 genomic DNA by PCR using a mixture of proof-reading (*Pfu*) and non-proof-reading (*Tth*) DNA polymerases (Biotools) with primers CAT2-OE-For (5'-GACTGAATTCATGAGGATCTGTCATTCGAGAACTCTCTC-3') and CAT2-OE-Rev (5'-GACTCTCGAGTCATAACTTTGCTTTTCGTTTATTCTCATTTTC-3'). A fragment of about 2 kb was obtained, purified and subcloned into the pGEM-T vector, yielding the pGEM-T-CAT2 construct. To enable cloning into the pHVX2 plasmid, an *EcoRI* site (underlined in the forward primer) immediately 5' of the first ATG start

codon (in boldface type) of the *CAT2* gene, and a *XhoI* site (underlined in the reverse primer) were introduced in the same PCR.

To overexpress VIN13 *CAT2* in *S. cerevisiae*, a 2013-nt DNA fragment containing *CAT2* was obtained from plasmid pGEM-T-CAT2 after digestion with *EcoRI* and *XhoI*. This fragment was then purified and subcloned into the *S. cerevisiae* expression plasmid pHVX2, previously digested with *EcoRI* and *XhoI*, to generate the pHVX2-CAT2^{mit} construct. The VIN13 *CAT2* cDNA fragment was sequenced (Fig. 31). The full-length open reading frame (2013 nt) encodes a mitochondrial precursor protein of 670 amino acids with a molecular mass of 77 kDa. Similar to rat CrAT, the N-terminal end of the precursor protein has a sequence of 22 amino acids (mitochondrial targeting signal or MTS) before the second methionine, which is the first amino acid in peroxisomal Cat2p (Cat2p per.). In addition to the MTS, the encoded protein possesses a PTS-like tripeptide “AKL” at its C-terminus. Since the MTS overrules the PTS, the protein encoded by the pHVX2-CAT2^{mit} construct will be located in the mitochondrial matrix (mitochondrial Cat2p or Cat2p mit.).

It has been shown that the deletion of both the MTS and PTS motifs results in a protein that localises in both peroxisomes and cytosol (Elgersma, 1995). Therefore, in order to colocalize carnitine and alcohol acetyltransferase activities in the cytosol, we produced the pHVX2-CAT2^{cyt} construct, in which the PTS and the first 22 amino acids of *CAT2* were deleted. Primers CAT2ΔN.for (5'-GACTGAATTCATGCATTCGGCCATTGTCAATTACTC-3') and CAT2ΔC.rev (5'-GACTCTCGAGTCATTTTCGTTTATTCTCATTTTCCAAG-3') were used to amplify VIN13 genomic DNA. The forward primer introduces an *EcoRI* site (underlined) immediately 5' of the second start codon (in boldface type) of *CAT2* and the reverse primer introduces a *XhoI* site (underlined) immediately after the stop codon (in boldface type). The protein encoded by the pHVX2-CAT2^{cyt} construct—named cytosolic Cat2p or Cat2p cyt—will be located in both the peroxisomes and cytosol.

Results

→ Cat2p mit.
ATGAGGATCTGTCAATTCGAGAACTCTCTCAAACCTAAAGGATCTTCCGATAACGTCAAGG 60
M R I C H S R T L S N L K D L P I T S R

AGAGCAATGCATTTCGGCCATTGTCAATTACTCCACCCAAAAGGCCCAATTTCCCGTAGAG 120
R A M H S A I V N Y S T Q K A Q F P V E

ACAAATAATGGGGAACACTATTGGGCGGAAAAGCCGAACAAATCTACCAGAACAAAAGG 180
T N N G E H Y W A E K P N K F Y Q N K R

CCCAATTTTCAAGGCATTACCTTTGCTAAACAACAAGAATTACCATCATTACCCGTGCC 240
P N F Q G I T F A K Q Q E L P S L P V P

GAATTGAAGTCTACACTTGACAAGTATTTGCAAACCATCCGCCATTTTGCAATGGTGTA 300
E L K S T L D K Y L Q T I R P F C N G V

GAAACTTTTGAAAGACAGCAGCTGTTATGTAAAGACTTCTCGGAGCACATGGGGCCTATC 360
E T F E R Q Q L L C K D F S E H M G P I

TTACAAGACCGGTTGAAAGAGTATGTCAACGATAAAAGAACTGGATGGCCAAGTTTTGG 420
L Q D R L K E Y V N D K R N W M A K F W

GATGAACAATCCTATTTACAATACAACGATCCCATTTGCCATACGTCTCTTATTTTTAT 480
D E Q S Y L Q Y N D P I V P Y V S Y F Y

TCTCATATGCCATTACCGAATCATTATCGAAGATCGATAATGATCCTTTGATTAAGGCT 540
S H M P L P N H L S K I D N D P L I K A

ACTGCGATTATCTCAACCGTGGTTAAATTCATCGAAGCTATTAAGATGAATCTTTACCC 600
T A I I S T V V K F I E A I K D E S L P

GTAGAAATTATCAAAGGTATGCCATTTGTATGAATAGTTTTTTCATTGATGTTAACACT 660
V E I I K G M P F C M N S F S L M F N T

TCGAGATTGCCTGGTAAGCCAGAGGATAACCAAGATACAAATATTTTTTATTCAGTTTAT 720
S R L P G K P E D N Q D T N I F Y S V Y

GAGAACAACCTTGTAACCTATCGCTTATAAAGGGAAGTTTTACAAACTGATGACCCATGAC 780
E N N F V T I A Y K G K F Y K L M T H D

GGGAATGACAAACCGCTTTCCGAAAACGAAATCTGGAGGCAACTGTACTCTGTGGTATTC 840
G N D K P L S E N E I W R Q L Y S V V F

CAAGGATCGCAGTCCGATCCCAAACCTAGGTGGCATTGGTTCTCTCACCTCTTTACCTCGT 900
Q G S Q S D P K L G G I G S L T S L P R

GATCAATGGCGTGAAGTACATATGGAGCTTATGAAAGATCCTATTTCTCAGGATTCACTA 960
D Q W R E V H M E L M K D P I S Q D S L

GAAACAATCCATAAGTCTTCCTTTATGCTATGTTGGATCTTGACCAATCCCCTGTCACT 1020
E T I H K S S F M L C L D L D Q S P V T

TTGGAAGAAAAGTCAAGAAATGCTGGCACGGTGATGGTATTAACAGATTCTACGATAAG 1080
L E E K S R N C W H G D G I N R F Y D K

TCTTTACAGTTCTGGTCACCGGTAATGGTTCATCAGGTTTCTTAGCTGAACACTCGAAG 1140
S L Q F L V T G N G S S G F L A E H S K

Results

ATGGATGGTACGCCAACATTGTTTTTAAATAACTACGTTTGTGGCAGTTGAATAAACTA M D G T P T L F L N N Y V C R Q L N K L	1200
GATGTGGATGACTTCATGAGAAAAGTAATTACGCCATCATCTACGGTGGCAATGAAACCT D V D D F M R K V I T P S S T V A M K P	1260
ATGGAAGTGCCTTCATTATCACACCGAAGATTCATAAAGCAATCGAATCTGCCCAACTA M E L P F I I T P K I H K A I E S A Q L	1320
CAATTTAAGGAAACAATTGGTGAGCATGACCTACGTGTTTGGCACTACAACAAATACGGA Q F K E T I G E H D L R V W H Y N K Y G	1380
AAAACGTTTATAAAACGCCATGGCATGTCACCTGATGCATTTATTCAACAAGTTATCCAA K T F I K R H G M S P D A F I Q Q V I Q	1440
CTGGCGGTTTTCAAATATCTGAAACGACAACCTACCAACTTACGAGGCTGCTTCCACGAGA L A V F K Y L K R Q L P T Y E A A S T R	1500
AAATACTTCAAAGCCGCTACTGAAACTGGTAGATCTGTGTCCACCGCTTCCCTAGAATTT K Y F K G R T E T G R S V S T A S L E F	1560
GTTTCTAAATGGCAAATGGCGATGTTCTATTGCAGAAAAGATTCAGGCTTTGAAACAT V S K W Q N G D V P I A E K I Q A L K H	1620
TCTGCAAAAGAGCATTCTACGTACCTGAGAAATGCTGCAAATGGTAATGGTGTGATCGT S A K E H S T Y L R N A A N G N G V D R	1680
CATTTCTTCGGTCTAAAGAATATGCTAAAATCTAATGATGACCAAATTCGCCCTTTTC H F F G L K N M L K S N D D Q I P P L F	1740
AAAGATCCCTTATTTAATTATTCTTCAACTTGGTTGATCTCCACATCTCAACTATCTTCG K D P L F N Y S S T W L I S T S Q L S S	1800
GAATATTTTGACGGTTATGGTTGGTCCCAAGTAAATGACAACGGGTTTGGACTGGCATA E Y F D G Y G W S Q V N D N G F G L A Y	1860
ATGTTGAATAACGAGTGGCTGCATATCAATATTGTCAACAAACCAGCCAAGAGTGGAGCC M L N N E W L H I N I V N K P A K S G A	1920
AGTGTTAACAGATTACACTATTATTTATCTCAAGCTGCTGATGAAATTTTGGACGCCTTG S V N R L H Y Y L S Q A A D E I F D A L	1980
GAAAATGAGAATAAACGAAAAGCAAAGTTA TGA E N E N K R K <u>A K L</u> *	2013

Fig. 31. **cDNA and amino acid sequence of VIN13 *CAT2***. Boxed nucleotides correspond to the first start codon as well as the stop codon, TGA. The second start codon is underlined. In the amino acid sequence, the peroxisomal targeting signal (PTS), AKL, is underlined. The coding sequence comprises nt 1-2013. Cat2p mit: mitochondrial CrAT.

11.3. OVEREXPRESSION OF *CAT2* IN *S. CEREVISIAE*

Plasmids pHVX2, pHVX2-*CAT2*^{mit}, and pHVX2-*CAT2*^{cyt} were transformed into a laboratory strain of *S. cerevisiae*, FY23, yielding the strains FY23(pHVX2), FY23(*CAT2* mit) and FY23(*CAT2* cyt), respectively. Strains FY23(*CAT2* mit) and FY23(*CAT2* cyt) overexpress mitochondrial and cytosolic Cat2p, respectively; FY23(pHVX2) was used as a control strain.

To confirm *CAT2* overexpression, carnitine acetyltransferase activity was measured in cell lysates of the transformed yeast grown on glucose (Fig. 32). Carnitine acetyltransferase activity was undetectable in yeast cells overexpressing the pHVX2 vector alone, since endogenous CrAT activity is not induced in glucose (Elgersma, 1995). Activity in FY23(*CAT2* mit) and FY23(*CAT2* cyt) strains was 62 and 298 nmol·min⁻¹·mg protein⁻¹, respectively.

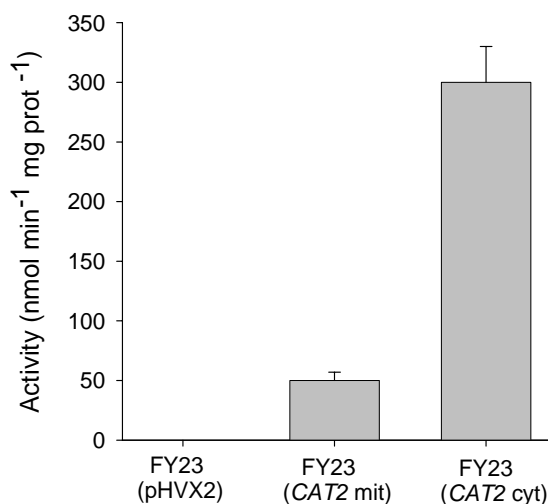


Fig. 32. **Carnitine acetyltransferase activity in FY23 strains overexpressing *CAT2*.** Protein extracts from yeast overexpressing *CAT2* were assayed for activity with acetyl-CoA. Results are shown as the mean \pm S.D. of three independent experiments.

11.4. EFFECT OF *CAT2* OVEREXPRESSION ON THE PRODUCTION OF VOLATILE FLAVOUR COMPOUNDS

FY23(pHVX2), FY23(*CAT2* mit), and FY23(*CAT2* cyt) strains were used for a series of fermentations of a synthetic medium containing 8% glucose and supplemented with L-carnitine (100 mg/L). During these fermentations, each strain's production of volatile compounds was analyzed by GC/MS and compared to that of the respective empty-vector control strain. Fermentations were performed as described in Materials and Methods (Section 5) and samples were taken for analysis after 4 and 7 days of fermentation. In addition to the concentration of volatile flavour compounds, sugar consumption was also measured. After 4 days of growth, virtually all of the sugar had been fermented.

The results of the GC/MS analysis are given in Table 14. The levels of ethyl acetate produced during fermentation with FY23(*CAT2* mit) and FY23(*CAT2* cyt) strains were significantly reduced ($p \leq 0.05$) after 7 days of fermentation when compared to the control strain (Fig. 33). The levels of 3-methyl butyl acetate (isoamyl acetate) were also significantly diminished when mitochondrial Cat2p was overexpressed, but this was not the case with cytosolic Cat2p (Fig. 33). The other acetate ester compounds, 2-methyl propyl acetate, 2-methyl butyl acetate and phenylethyl acetate, were not significantly affected by the overexpression of *CAT2*.

As for C₃-C₁₂ fatty acid ethyl esters, overexpression of cytosolic Cat2p had almost no effect on the levels of these compounds, whereas overexpression of mitochondrial Cat2p resulted in a modest, although significant, decrease in the concentrations of ethyl butanoate (after 4 and 7 days of fermentation), ethyl hexanoate (4 and 7 days), and ethyl octanoate (4 days) (Fig. 33).

Overexpression of mitochondrial Cat2p caused a 50% increase of 2-methyl-propanol formation compared to that in control cells (Fig. 33). The other alcohol compounds, 2-phenylethanol, 2-methyl butanol and 3-methyl-butanol, were not significantly affected by the overexpression of *CAT2*.

Results

Regarding the production of organic acids, overexpression of *CAT2* produced a decrease in the levels of these compounds. The formation of organic acids, such as 3-methyl butanoic, hexanoic, octanoic and decanoic acids, was significantly decreased when the cytosolic or mitochondrial *Cat2p* isoforms were overexpressed.

Component	Conc. (mg / liter)					
	4 days fermentation			7 days fermentation		
	FY23 (pHVX2)	FY23 (<i>CAT2</i> cyt)	FY23 (<i>CAT2</i> mit)	FY23 (pHVX2)	FY23 (<i>CAT2</i> cyt)	FY23 (<i>CAT2</i> mit)
Ethyl acetate	8.0	6.3	6.8	10.6	8.1	8.6
2-methyl propyl	0.005	0.005	0.005	0.006	0.005	0.006
2-methyl butyl acetate	0.014	0.012	0.012	0.011	0.012	0.011
3-methyl butyl acetate	0.076	0.068	0.051	0.065	0.059	0.049
Phenylethyl acetate	0.015	0.016	0.011	0.015	0.013	0.013
Ethyl propanoate	0.029	0.027	0.026	0.030	0.026	0.027
Ethyl 2-methyl	0.002	0.002	0.003	0.003	0.002	0.003
Ethyl butanoate	0.067	0.061	0.052	0.066	0.054	0.051
Ethyl 2-methyl	u.d.	u.d.	u.d.	u.d.	u.d.	u.d.
Ethyl hexanoate	0.24	0.21	0.18	0.16	0.15	0.12
Ethyl octanoate	0.13	0.088	0.091	0.12	0.11	0.10
Ethyl decanoate	0.040	0.034	0.032	0.035	0.034	0.029
Ethyl dodecanoate	0.002	0.002	0.002	u.d.	u.d.	u.d.
Ethyl lactate	5.4	4.8	5.2	5.4	5.4	5.6
2-phenyl ethanol	5.0	4.6	4.7	6.0	4.9	5.9
2-methyl propanol	5.9	5.8	8.9	6.8	5.9	9.1
2-methyl butanol	5.1	5.7	6.9	6.9	5.6	6.7
3-methyl butanol	23.0	21.0	21.5	24.1	18.9	23.4
Acetic acid	370	420	422	419	355	409
2-methyl propanoic	0.47	0.46	0.56	0.62	0.42	0.65
2-methyl butanoic acid	0.084	0.068	0.075	0.094	0.079	0.099
3-methyl butanoic acid	0.11	0.081	0.074	0.10	0.075	0.094
Butanoic acid	21.0	20.5	20.4	20.8	20.2	20.6
Hexanoic acid	1.6	1.6	1.3	2.3	1.8	1.6
Octanoic acid	4.3	3.2	2.8	6.2	4.6	4.7
Decanoic acid	3.3	3.0	2.5	2.9	2.2	2.1

Table 14. **GC/MS measurement of volatile compounds produced by *CAT2*-overexpression strains after 4 and 7 days of fermentation.** Results are shown as the averages of six independent fermentations. Values shown in bold are significantly different ($P \leq 0.05$) from the control strain FY23(pHVX2). The standard deviation did not exceed 20% for any of the values.

Results

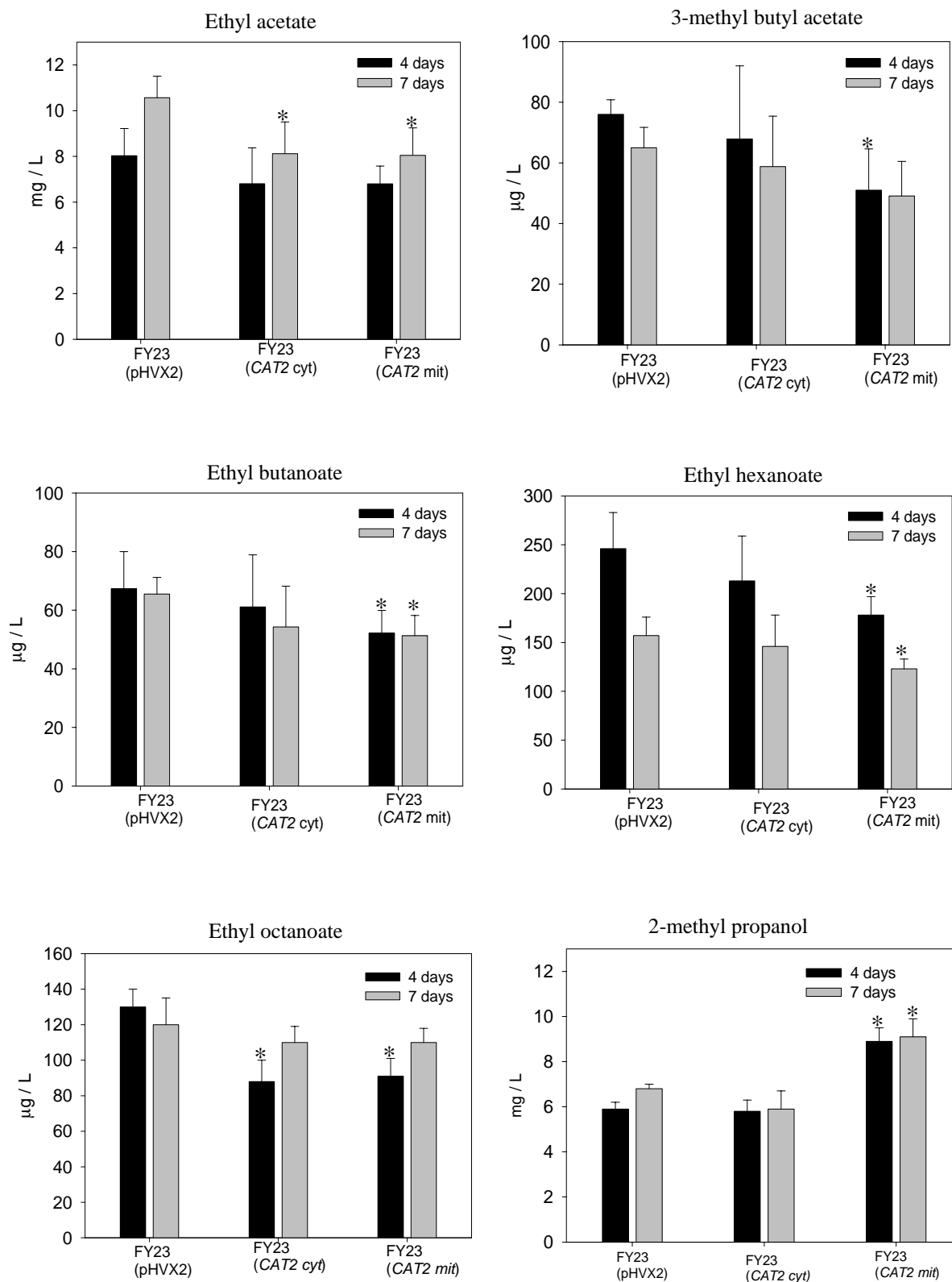


Fig. 33. **Concentrations of representative volatile esters and alcohols.** Data are presented as the mean \pm S.D. of six independent experiments. * $P < 0.05$; compared with the control strain FY23(pHVX2).

11.5. EFFECT OF OVEREXPRESSING A MUTANT *CAT2* ON THE PRODUCTION OF VOLATILE FLAVOUR COMPOUNDS

Through the experiments performed previously (Section 6.2.1.), we converted rat CrAT into a pseudo rat COT by modifying a single amino acid (mutation of Met⁵⁶⁴ to Gly in CrAT). Taking into consideration our experimental results and the fact that yeast cells are devoid of COT and CPT activities, we attempted to change yeast Cat2p acyl-CoA specificity from short-chain acyl-CoAs to medium-chain acyl-CoAs by site-directed mutagenesis. The objective of this mutagenesis study was to investigate the effect of a novel carnitine acyltransferase activity on the production of volatile esters. If this mutated *CAT2* were to be overexpressed in yeast, the levels of medium-chain acyl-CoAs would be influenced, and therefore, so would the levels of medium-chain fatty acid esters such as ethyl hexanoate or ethyl octanoate. These medium-chain fatty acid ethyl esters, which have “sour-apple” aromas, are also important for the overall bouquet of wine.

We performed an amino acid alignment of 16 carnitine acyltransferases, including *S. cerevisiae* (CACP_YEAST) and *Candida tropicalis* (CACP_CANTR) Cat2p (Fig. 34). The equivalent amino acids of rat CrAT Met⁵⁶⁴ are Tyr⁶⁰⁶ in the budding yeast and Trp⁵⁶² in *C. tropicalis*. The presence of two bulky residues at this position in yeast carnitine acetyltransferases supported the hypothesis that these residues could be involved in acyl-CoA specificity in yeast, since the larger side chain of Tyr⁶⁰⁶ and Trp⁵⁶² would prevent access of long-chain acyl-CoAs to the enzyme's active site.

Therefore, we decided to mutate the bulky Tyr⁶⁰⁶ to the tiny Gly in VIN13 *CAT2*. The mutation was introduced using a PCR-based mutagenesis procedure using the pHVX2-CAT2^{cyt} as template and the primers CAT2-Y606G.for and CAT2-Y606G.rev, yielding the pHVX2-CAT2^{Y606G-cyt} construct. The plasmid was then transformed into the *S. cerevisiae* strain FY23, yielding FY23(*CAT2* Y606G cyt).

```

CACP_YEAST 600 SEYFD...GYGWSQVNDNGFGLAY
CACP_CANTR 556 SEFFQ...SWGWSQVIDDGFGLAY
CACP_HUMAN 556 AKTDC...VMFFGPVVPDGYGVCY
CACP_MOUSE 559 AKTDC...VMFFGPVVPDGYGICY
CACP_COLL 559 AKTDC...VMCFGPVVPDGYGICY
OCTC_HUMAN 547 GYLRV...GGVVVPMVHNGYGFFY
OCTC_RAT   547 GYLRI...GGVVVPMVHNGYGFFY
OCTC_BOVIN 547 GYLRV...GGVMVPMVHNGYGFFY
CPTM_RAT   704 NHLGA...GGGFGPVADHGYGVSY
CPTM_HUMAN 704 NHLGA...GGGFGPVADHGYGVSY
CPT1_RAT   704 DYVSC...GGGFGPVADHGYGVSY
CPT1_MOUSE 695 DYVSC...GGGFGPVADHGYGVSY
CPT1_HUMAN 704 EYVSS...GGGFGPVADHGYGVSY
CPT2_RAT   594 SPAVS...LGGFAPVVPDGFGIAY
CPT2_MOUSE 594 SPAVS...LGGFAPVVPDGFGIAY
CPT2_HUMAN 594 SPAVN...LGGFAPVVSQGFVGVI

```

Fig. 34. **Alignment of representative sequences of carnitine acyltransferases.** ClustalW was used to align the amino acid sequences of 16 carnitine acyltransferase enzymes: CrAT (CACP) from yeast, *C. tropicalis*, human, mouse and pigeon; L-CPT I (CPT1) from rat, mouse and human; M-CPT I (CPTM) from human, and rat; CPT II (CPT2) from rat, mouse and human; and COT (OCTC) from human, rat and cattle. Residues are coloured according to conservation. The position of the conserved residue is indicated according to acyl-chain length specificity (Met⁵⁶⁴ for mammalian CrAT, Tyr⁶⁰⁶ for yeast CrAT (Cat2p) and a glycine for COT and CPT).

To examine whether the amino acid Tyr⁶⁰⁶ plays an important role in determining fatty acyl chain-length specificity in yeast Cat2p, carnitine acetyltransferase activity in cell lysates of the FY23(*CAT2* Y606G cyt) strain was tested for acyl-CoAs substrates of various lengths and compared with the FY23(*CAT2* cyt) strain (Fig. 35). Cytosolic Cat2p had exceptional selectivity for C₂-CoA, whereas C₃- or C₄- rather than C₂-CoA is the optimal substrate for mammalian CrATs. Activity with C₄-CoA was only 15% of that with C₂-CoA, and chain lengths longer than C₄-CoA showed no detectable activity.

Contrary to our expectations, mutant Y606G maintained the same substrate preference as the wild-type enzyme and did not display enhanced activity with medium- or long-chain acyl-CoAs. The results indicate that mutation of Tyr⁶⁰⁶ to Gly has no effect on acyl-CoA selectivity.

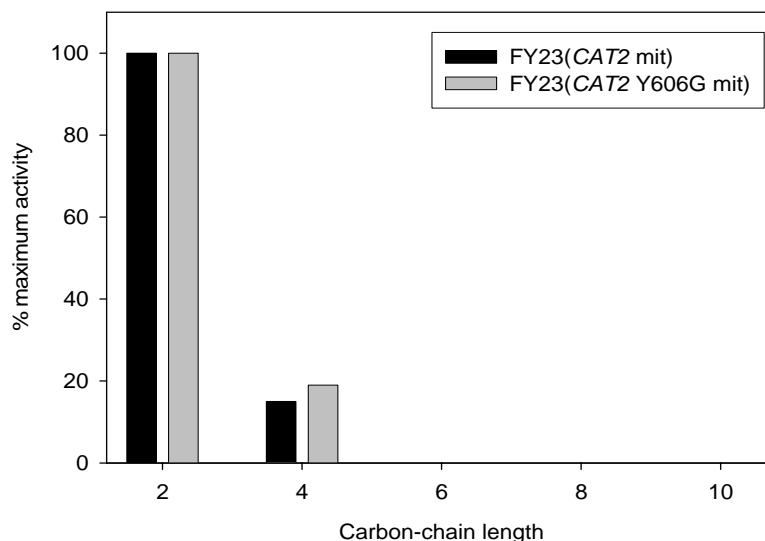


Fig. 35. **Carnitine acyltransferase activity of yeast cells expressing cytosolic Cat2p and mutant Y606G.** Lysates from yeast expressing cytosolic Cat2p (FY23(CAT2 cyt)) and mutant Y606G (FY23(CAT2 Y606G cyt)) were assayed for activity with acyl-CoAs of different carbon-chain lengths, ranging from acetyl- to decanoyl-CoA. Results are expressed as the relative acyl-CoA activity with regard to acetyl-CoA activity (scaled to 100).

The FY23(CAT2 Y606G cyt) strain was used for a series of fermentation experiments, as described above (Section 11.4). After 4 days of fermentation, the production of volatile compounds was analysed by GC/MS and compared to that of the respective empty-vector control strain FY23(pHVX2).

The results of the GC/MS analysis are shown in Table 15. The levels of acetate esters, medium-chain fatty acid ethyl esters, alcohols and organic acids, were not significantly affected by the overexpression of mutant Y606G. These results indicate that mutation of Tyr⁶⁰⁶ to Gly in Cat2p has no effect on the production of volatile flavour compounds.

Results

Component	Conc. (mg /liter)	
	FY23 (pHVX2)	FY23 (<i>CAT2</i> Y606G cyt)
Ethyl acetate	3.3	3.5
2-methyl propyl acetate	0.002	0.002
3-methyl butyl acetate	0.045	0.049
Phenylethyl acetate	0.011	0.012
Ethyl propanoate	0.016	0.017
Ethyl 2-methyl propanoate	0.001	0.001
Ethyl butanoate	0.045	0.045
Ethyl hexanoate	0.17	0.17
Ethyl octanoate	0.047	0.048
Ethyl decanoate	0.015	0.016
Ethyl dodecanoate	0.009	0.010
2-phenylethanol	5.4	5.4
2-methyl propanol	4.6	4.6
2-methyl butanol	4.3	4.5
3-methyl butanol	17.1	17.4
Acetic acid	313	312
2-methyl propanoic acid	0.67	0.65
2-methyl butanoic acid	0.097	0.095
3-methyl butanoic acid	0.15	0.14
Hexanoic acid	1.1	1.1
Octanoic acid	1.9	1.9
Decanoic acid	2.7	2.8

Table 15. **GC/MS measurement of volatile compounds produced by the *CAT2*-overexpression strain FY23(*CAT2*Y606G cyt) after 4 and 7 days of fermentation.** Results are shown as the averages for six independent fermentations. Values shown in bold are significantly different ($P \leq 0.05$) from the wild-type strain FY23 (pHVX2). The standard deviation did not exceed 20% for any of the values.